EXPERIMENTAL DETERMINATION OF THE INTERFACIAL TENSION OF BINARY SYSTEMS

By

Michael Brant Miller

Bachelor of Science

Oklahoma State University

Stillwater, Oklahoma

1970

Submitted to the Faculty of the Graduate College
of the Oklahoma State University
in partial fulfillment of the requirements
for the Degree of
MASTER OF SCIENCE
May, 1972

EXPERIMENTAL DETERMINATION OF

THE INTERFACIAL TENSION OF

BINARY SYSTEMS

Thesis Approved:

R. N. Maddox

Thesis Adviser

John B. West

D. Dunham

Dean of the Graduate College

PREFACE

Experimental information on the interfacial tension of multi-component systems is uncommon in the available literature. An experimental apparatus was developed to obtain such information over a wide range of conditions. The apparatus was employed to investigate mixtures of normal-pentane in para-xylene and acetone in water. The results of consideration of the two binary systems were compared to typical correlation predictions to assess the difficulties to be expected in the use of predictive methods.

I wish to express my gratitude to Dr. R. N. Maddox for the guidance provided by him as my thesis adviser. I would also like to thank Drs. John H. Erbar and V. K. Mathur for their advice on technical matters. I would especially like to thank the members of Heat Transfer Research Incorporated for the financial incentive for this work, and my wife, Suzie, for her perserverance.

TABLE OF CONTENTS

LIST OF TABLES

LIST OF FIGURES

LIST OF SYMBOLS

Major Symbols

English Letters

b	- radius of curvature of drop at origin
d_e	- drop equatorial diameter
d_s	- selected plane diameter
g	- gravitational acceleration
H	- shape dependent parameter
M	- molecular weight
m	- correlative parameter
p	- pressure
	pressure difference across interface
$[P]$	- parachor
R and R'	- principal radii of curvature for curved surfaces
S	- liquid drop shape factor
T	- temperature
V	- volume
v	- volume fraction
w	- acentric factor
x	- molar concentration in liquid phase
y	- molar concentration in vapor phase

Greek Letters

α	- Reidel critical parameter
β	- drop shape parameter
γ	- interfacial tension
δ	- uncertainty in measured quantity
ρ	- density

Subscripts

A	- component A
B	- component B
c	- critical property
i	- component number
l	- liquid phase
R	- reduced property
s	- at surface or in surface layer
v	- vapor phase

CHAPTER I

INTRODUCTION

As interfacial tension is the physical property which defines the nature of the interface between two phases, it is of interest to those who must design equipment for multiphase operations. With the needs of these individuals for adequate information on interfacial tension in mind, this study was undertaken.

The goals of the study were to produce an apparatus through which the interfacial tension of a system could be accurately evaluated over a wide range of conditions and to utilize that equipment to investigate systems of immediate concern. A primary consideration was that the equipment produced should have accurate means to evaluate those variables chosen to be fixed.

The means of approach to interfacial tension determination was through the pendant drop method. Experimental measurements were made on binary mixtures of normal-pentane in para-xylene and acetone in water. Component concentrations were varied for each system. As interfacial tension was of concern, the liquid drops were suspended in their corresponding equilibrium vapor.

CHAPTER II

LITERATURE SURVEY

Boundary tension can be considered to be a measure of the free energy per unit surface area at a fluid phase interface, or the force exerted by an interphase surface of unit length. In accordance with common usage, this work will adopt the definition by Andreas et al. (2) of surface tension as the boundary tension between a liquid and a gas or vapor. The term interfacial tension will be held to imply the existence of an equilibrium between the vapor and the liquid. Though more restrictive, this is compatible with the definition by Hough et al. (9) of interfacial tension as a measure of the specific free energy between two phases of different composition.

For this work, the system of concern is to be a droplet of liquid whose composition is known, suspended from a capillary tip and immersed in its corresponding equilibrium vapor. This approach to interfacial tension determination is referred to as the pendant drop method.

Deam (4), following the approach of previous works, gives a mathematical description of the drop based on the Laplace and Young equation (1) for the pressure difference across the interface.

$$P = \gamma\left(\frac{1}{R} + \frac{1}{R'}\right) \qquad (1)$$

The expression arrived at by Deam for the surface tension, γ,

is given in equation (2).

$$\gamma = \frac{g(\rho_l - \rho_v)d_e^2}{H} \tag{2}$$

Associated with this expression are two shape dependent parameters S and H, given by equations (3) and (4).

$$S = \frac{d_s}{d_e} \tag{3}$$

$$\frac{1}{H} = -\frac{1}{\beta\left(\frac{d_e}{b}\right)^2} \tag{4}$$

The equatorial diameter is d_e, and d_s is the diameter of a selected plane at a distance d_e from the vertex of the drop, as shown in Figure 1. The radius of curvature of the drop at the origin is b, and β is a defined parameter given by the expression in equation (5). The phase densities are ρ_l and ρ_v, and g is the gravitational acceleration.

$$\beta = -gb^2 \frac{(\rho_l - \rho_v)}{\gamma} \tag{5}$$

Numerical tabulations of shape factor (S) as a function of shape parameter (1/H) are provided in a number of works. Those of Fordham (7), Niederhauser and Bartell (17), Mills (15), and Stauffer (24) were checked by Deam, who employed a method of successive approximations to perform the necessary integration. The values given by Deam were in substantial agreement with those of the work mentioned. Combination of these tables provided coverage of the useful range of drop shapes.

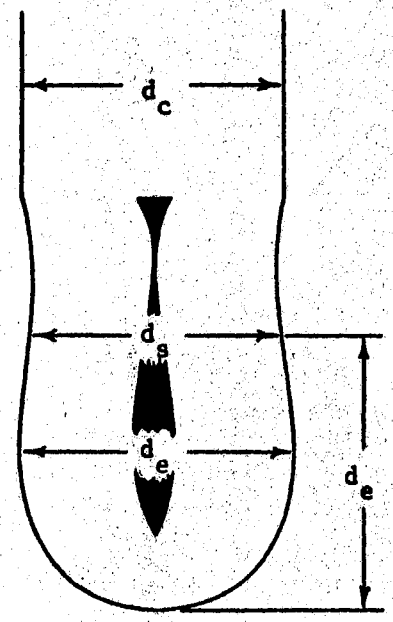

Figure 1. Pendant Drop Profile

The determination of the interfacial tension of a particular drop was to consist of obtaining a photograph of the drop, measuring the required drop diameters from the photographic negative, and calculating the shape factor, S. The shape parameter, 1/H, was then to be evaluated from the appropriate table and the interfacial tension calculated from equation (2).

According to Deam (4) and Niederhauser and Bartell (17), the pendant drop method is an absolute procedure. Thus it requires no calibration to a material of known interfacial tension. The accuracy of the method is determined primarily by the accuracy of the shape factor tables used and the quality of the photographs obtained of the drop. The latter is dependent upon the refinement of the optical system employed.

Predictive Correlations

For pure substances, a number of correlations were available for consideration. The approaches of Sugden (25), Reilly and Rae (22), and Brock and Bird (3) were to be evaluated in terms of their ability to predict the values of interfacial tension that were experimentally observed. Sugden proposed the parachor from consideration of the Ferguson and Macleod relationship of equation (6).

$$\frac{M \gamma^{1/4}}{\Delta \rho} = [P] \qquad (6)$$

The parachor, [P], was to be an additive function of the atoms and groups in the molecule. Quayle (19) gave a detailed tabulation of group contributions that was chosen for use with equation (6) to

predict interfacial tension for pure non-polar substances. Reilly and Rae expressed the parachor as a function of critical properties of the substance, as indicated in equation (7).

$$[P] = 0.41\, T_c^{1/4} V_c^{5/6} \tag{7}$$

The value of the parachor obtained through equation (7) was chosen to be used with equation (6) to predict interfacial tension for pure non-polar substances. The third predictive approach, that of Brock and Bird, gave the interfacial tension from equation (8).

$$\frac{\gamma}{T_c^{1/3} P_c^{2/3}} = (0.133\alpha_c - 0.281)(1 - T_R)^{11/9} \tag{8}$$

The term α_c was the Riedel critical parameter (21). This parameter was evaluated from equation (9) of Pitzer et al. (18).

$$\alpha_c = 5.808 + 4.93w \tag{9}$$

In cases where polar substances were of concern, the approach of Hakim et al. (8) used the expression given in equation (10) to arrive at the interfacial tension.

$$\gamma_R = (\gamma_R \Big| T_R = 0.6)\left(\frac{1-T_R}{0.4}\right)^{m(w,x)} \tag{10}$$

This approach was utilized to predict interfacial tension values for acetone and water. A more complete description of the approach is provided in Appendix C.

For mixtures of non-polar fluids, the approach of Weinaug and Katz (27) was chosen for consideration due to its applicability at elevated pressures. These authors gave the interfacial tension of a mixture as indicated in equation (11).

$$\gamma^{1/4} = \frac{\rho_l}{M_l}\Sigma x_i [P_i] - \frac{\rho_v}{M_v}\Sigma y_i [P_i] \qquad (11)$$

The tabulations of values for the parachor of the components that were provided in the work of Quayle (19) were used with this correlation.

Mixtures of polar fluids were to be considered through the correlation of Tamura et al. (26). Tamura gave the interfacial tension of the mixture as a function of the interfacial tensions of the pure components involved, as stated in equation (12).

$$\gamma^{1/4} = (1-v_s)\gamma_A{}^{1/4} + v_s\gamma_B{}^{1/4} \qquad (12)$$

The term v_s is the volume fraction of component B at the liquid surface, for which Tamura provided an expression relating v_s to the bulk concentration of component B. In his approach, Tamura considered component B as the polar organic substance in a solution with water, component A. The estimated error for the correlation was given to be within ten per cent for water solutions of ketones with less than six carbon atoms.

CHAPTER III

EXPERIMENTAL APPARATUS

The pendant drop apparatus assembled for this study is presented schematically in Figure 2. To facilitate explanation of its components and their function, the unit will be broken into five subsystems, each to be discussed separately.

The Cell and Temperature Control Subsystem

The cell, as depicted in Figure 3, consisted of two chambers; a liquid drop chamber containing the vapor phase, and a liquid chamber. The vapor space had a volume of fourteen cubic centimeters and was bounded at either end by a fused quartz window. The details of the window assembly are presented in Figure 4. The test pressure of the vapor cell was given by Deam (4) to be 1500 psia. The sample introduction subsystem terminated inside of the vapor space with the capillary from which the liquid drop was suspended.

The liquid chamber had a volume of 500 cc and was hydrostatically tested to 6000 psia. At the top of the chamber was a threaded fitting which joined the vapor and liquid spaces. A Conax iron-constantan thermocouple passed through the top of the liquid chamber to monitor cell temperature. The bottom of the chamber was fitted with lines leading to the pressure transducer and the sample discharge subsystem.

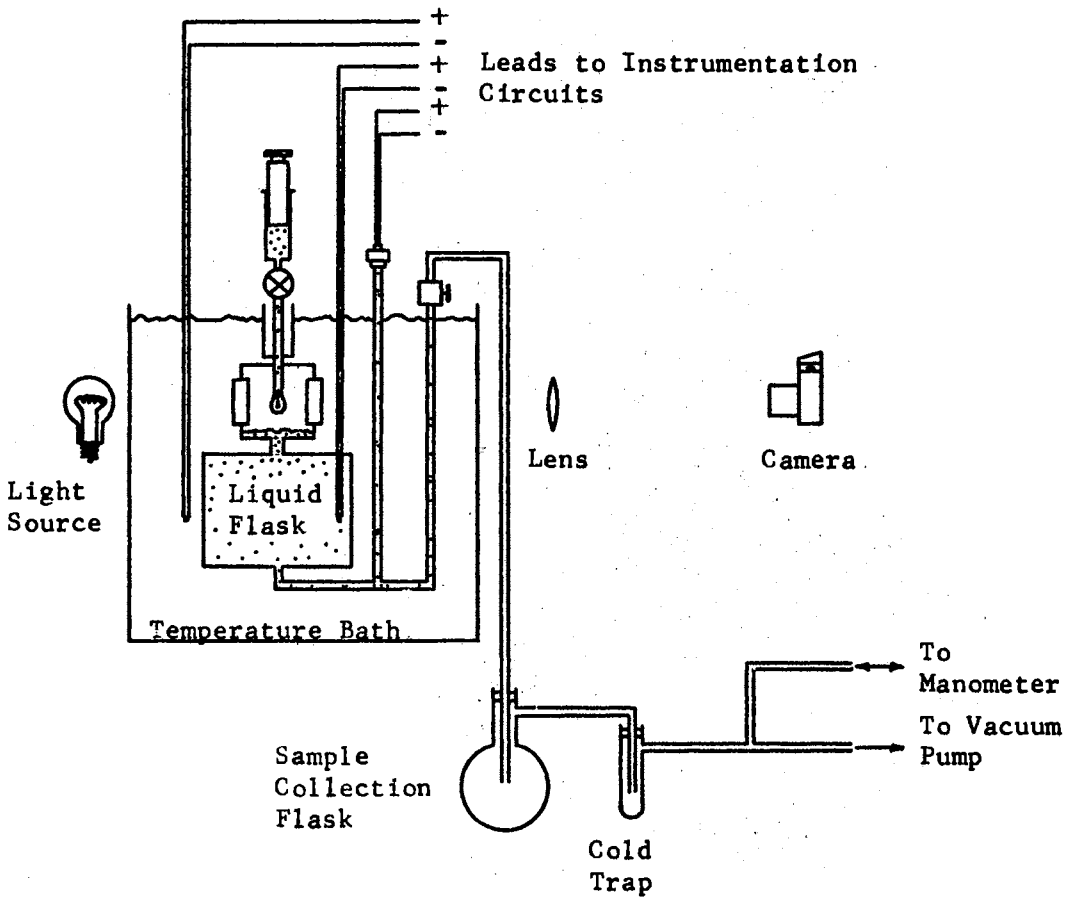

Figure 2. The Pendant Drop Apparatus

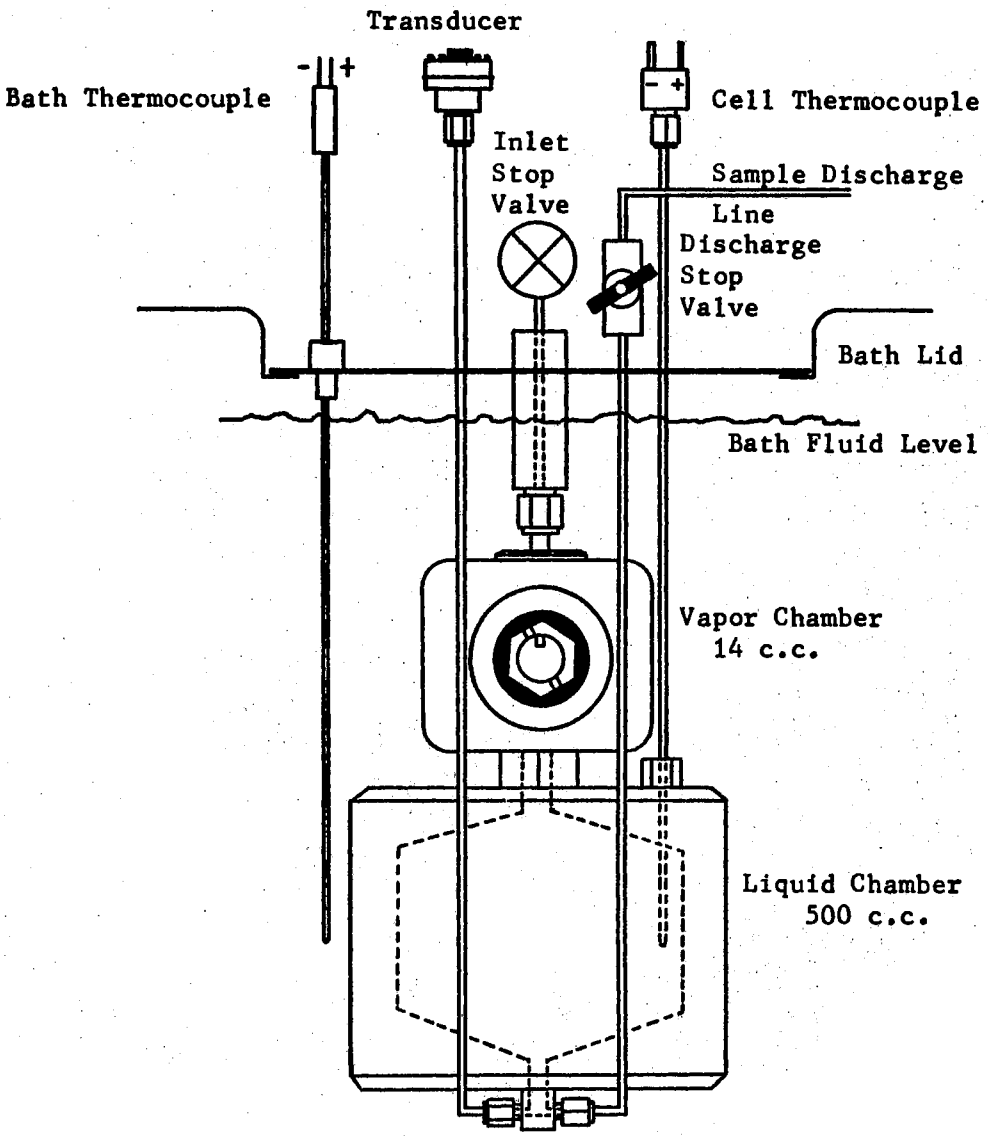

Figure 3. The Cell and Temperature Control Subsystem

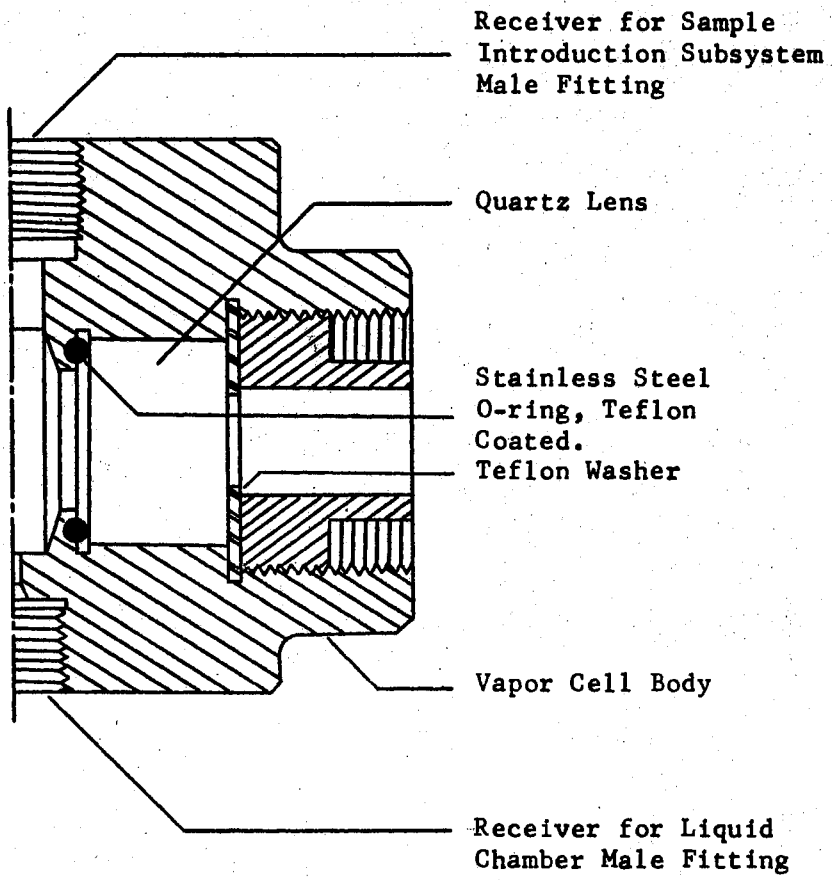

Figure 4. Vapor Cell Viewport Detail

The purpose of the vapor chamber was to contain the pendant liquid drop in an environment of its corresponding equilibrium vapor, and to provide the means by which the drop could be photographed. The liquid chamber contained 500 cc of a liquid with composition the same as that of the pendant drop. The purpose of the liquid reservoir was to fix the vapor composition prior to introduction of the liquid drop to the system. Calculations provided in Appendix A indicate that from 500 cc of binary liquid, 14 cc of equilibrium vapor could be formed with an associated change of liquid phase composition in the range of 0.005 mole per cent at 150°F., to 0.08 mole per cent at 393°F. Thus the liquid phase composition remained essentially fixed throughout the temperature excursion of a complete run.

The temperature bath was a Tamsen model TEV-70 of seventy liter capacity. The fluid used was General Electric silicone fluid, type SF 1154. The limits of the useful temperature range were determined by the bath fluid behavior. Below 120°F., the fluid was too viscous to be adequately circulated by the pump, and above 400°F., refractive index differences associated with thermal gradients in the fluid precluded photography. The cell was suspended from the lid of the bath on a support frame which, for clarity, has been omitted from Figure 3. The bath thermocouple was extended through the lid into the bath fluid to the same depth as the cell thermocouple.

The Instrumentation Subsystem

The monitoring devices consisted of three Conax iron-constantan thermocouples and a C.E.C. type 4-317 pressure transducer. The transducer response range was from 0 to 1000 psig, operating on a constant

five volt direct current input signal supplied by a Harrison Laboratories model 801-C power supply unit.

Output response of these devices was monitored on a Leeds and Northrup model 8686 millivolt potentiometer. The cell and bath thermocouples were calibrated against three reference temperatures. The reference temperatures used were the melting point of distilled water at 32°F., the boiling point of distilled water at 210.9°F. and an atomospheric pressure of 746 mmHg, and the melting point of pure tin at 449.4°F. The transducer was calibrated against a Budenberg dead weight gauge tester, number 2167. The calibration curves are presented in Appendix B, and the subsystem is depicted schematically in Figure 5.

The Sample Introduction Subsystem

To provide the driving force required to form the liquid drop at the capillary tip, a piston was driven by a vernier screw into a cylinder containing the liquid sample. The cylinder was outside of the temperature bath and the feed line from the cylinder to the cell was shielded from the bath fluid. The purpose of this shielding was to minimize the transfer of heat to the liquid in the feed line. With the feed line exposed to the bath fluid the liquid drops would alternately cascade from the tip or withdraw back into the feed line, independent of whether the inlet stop valve was open or closed. This erratic behavior was attributed to expansion and contraction of the liquid in the feed line as a result of bath temperature cycling. The addition of the heat shield controlled this response to the cycling at temperatures below 350° F. At higher temperatures the temperature

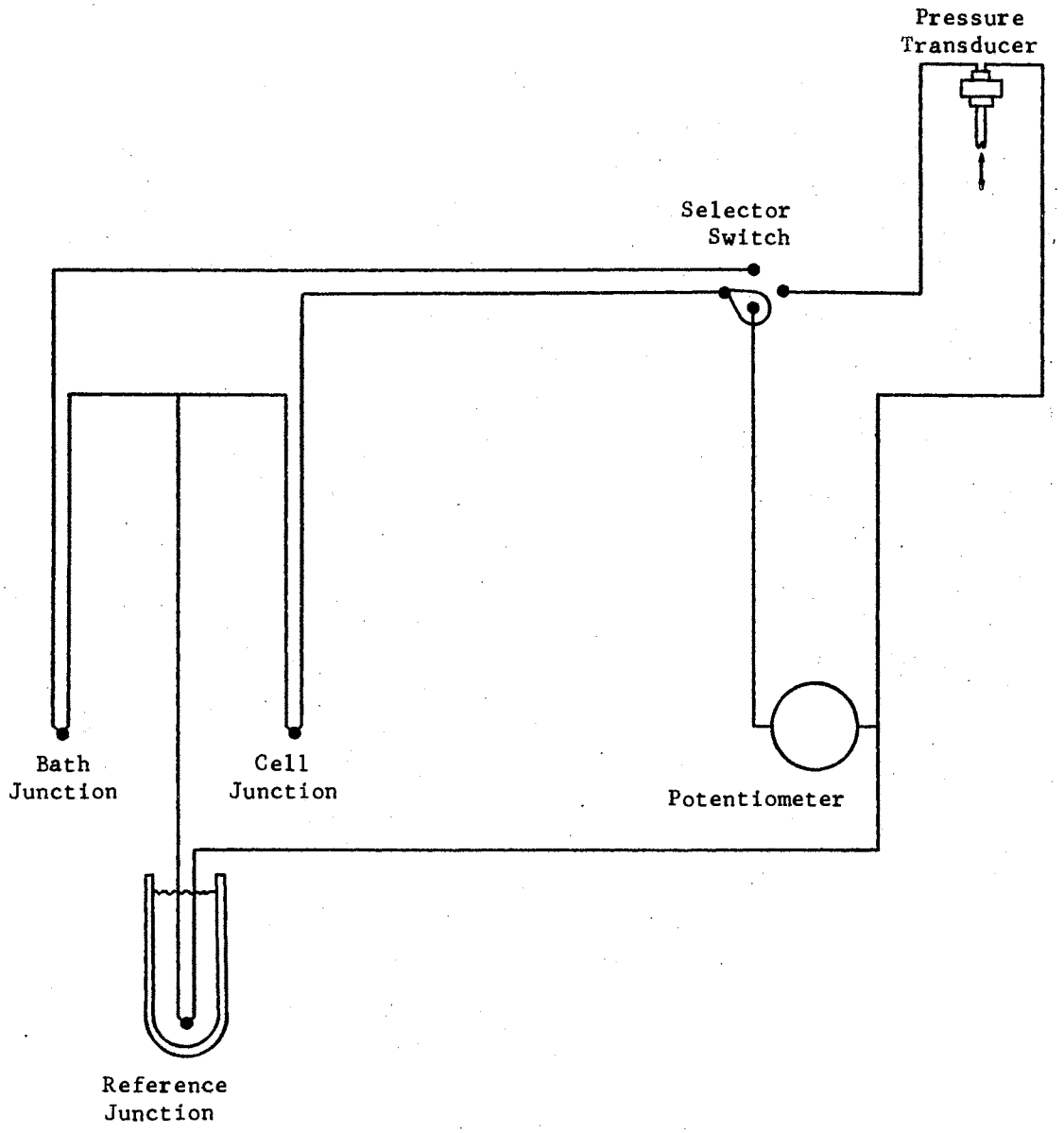

Figure 5. The Instrumentation Subsystem

cycling was seen to affect the liquid in the feed line, but to a lesser extent than with the line bare. The subsystem is depicted in Figure 6.

The Evacuation and Sample Discharge Subsystem

The evacuation subsystem utilized a Duo Seal model 1403 vacuum pump acting through a two liter vacuum flask to evacuate the cell prior to the introduction of a liquid sample. A fifty inch mercury filled U-tube manometer was located in the line to the vacuum pump to give indication of system pressure during evacuation. For sample removal following a run, the liquid from the cell was transferred to the vacuum flask. For liquids of low normal boiling point, a cold trap was installed between the collection flask and the manometer to prevent liquid from collecting in the lines to the manometer and vacuum pump. The use of a coil and copper line from the cell to the collection flask was intended to provide cooling prior to collection. Such cooling was desirable since the liquid in the cell was well above the normal boiling point at the time that it was discharged from the cell to the flask. The subsystem is shown in Figure 7.

The Optical Subsystem

A Cenco one hundred watt high pressure mercury arc lamp was directed through one window of the cell. The image of the drop, as seen through the other window, was projected through a double convex lens to a Konika model FS 35 millimeter single lens reflex camera. The film used was Kodak High Contrast Copy Film. The negatives obtained

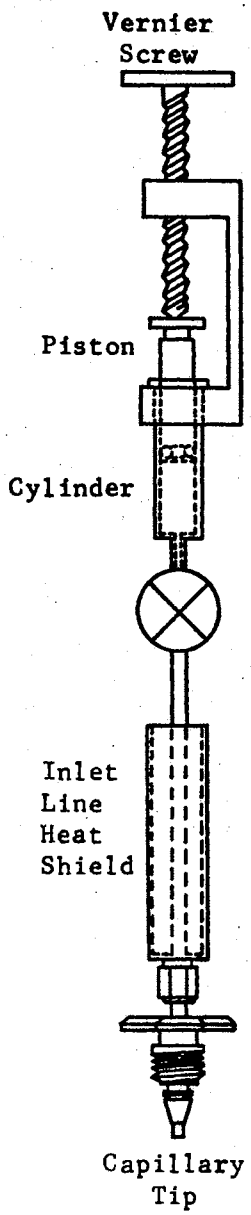

Figure 6. The Sample Introduction Subsystem

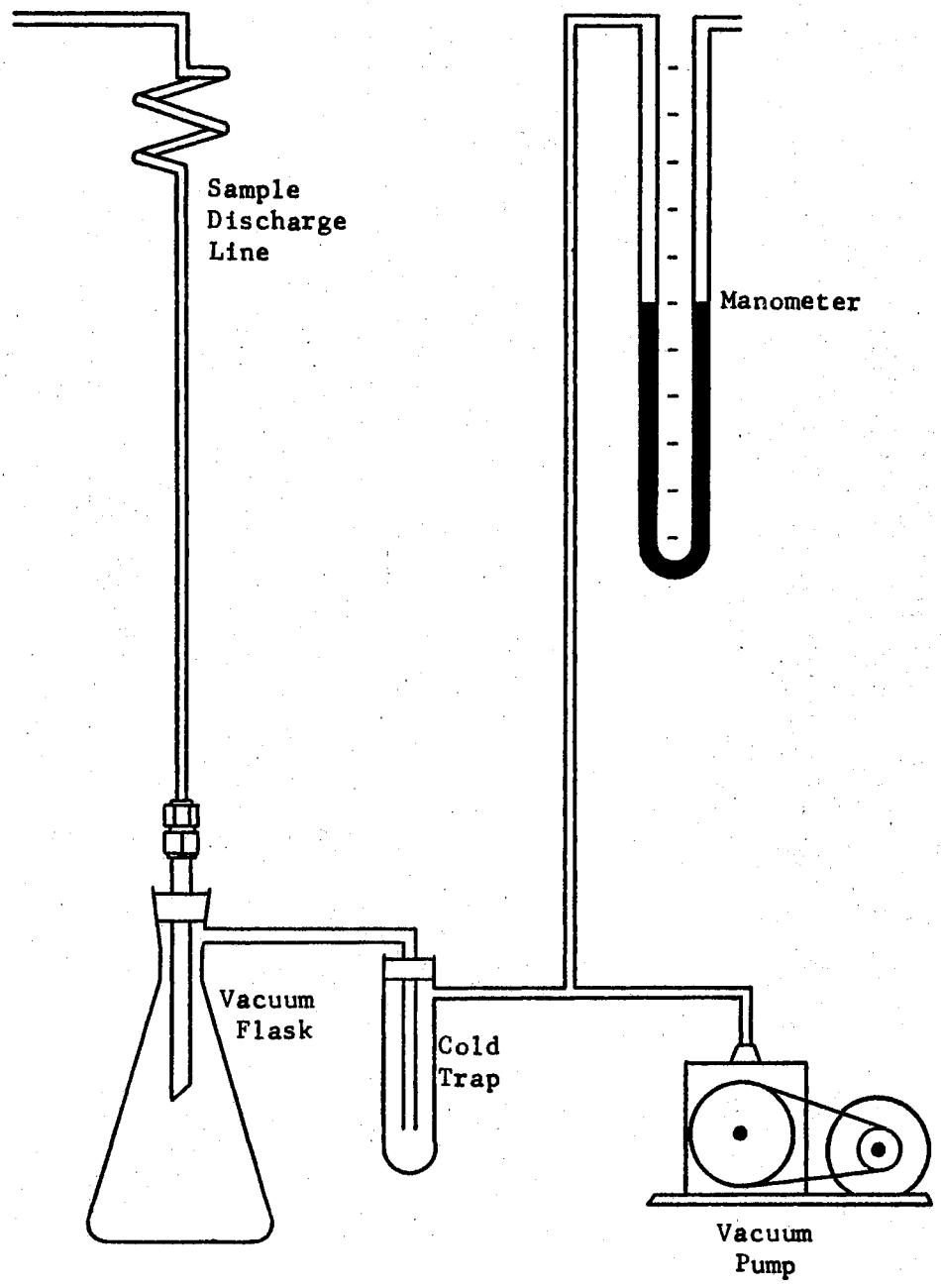

Figure 7. The Evacuation and Sample Discharge Subsystem

were projected on a Vanguard CD-11 motion analyzer for measurement of drop diameters. The arrangement of the optical subsystem can be seen in Figure 2.

CHAPTER IV

EXPERIMENTAL PROCEDURE

An experimental run was to consider liquid drops of a given composition at several selected temperatures. As a vapor-liquid equilibrium was to exist, pressure and, in cases where the system was a binary, vapor phase composition were variant with temperature. The systems and liquid phase compositions to be considered were normal-pentane in para-xylene of zero, ten, ninety, and one hundred per cent pentane, and acetone in water of zero, thirty, seventy, and one hundred per cent acetone. The materials from which these systems were prepared are as follows:

Component	Quality	Purity	Source
n-pentane	pure grade	99 mole % minimum	Phillips Petroleum Company
p-xylene	pure grade	99 mole % minimum	Phillips Petroleum Company
acetone (for pure samples)	Spectrophotometric 9010		J. T. Baker Chemical Company
acetone (for binary systems)	Spectranalyzed A-19		Fisher Scientific Company
water	single distilled		(local)

Liquid phase composition was determined from gravimetric evaluation at the time the samples were prepared. This composition was checked at various stages during the run by comparing the refractive index of a liquid sample from the cell with a curve of index of refraction as a function of composition. The curve was developed from the indices of refraction of several small samples which were prepared gravimetrically using a Mettler model B-6 balance.

Cell temperature was known from the output of the cell thermocouple. The existence of thermal equilibrium was assumed when the cell thermocouple attained a reasonably constant reading and the temperatures indicated by the cell and bath thermocouples were coincident. As temperature transitions were made rather slowly, equilibrium between the vapor and liquid phases was assumed to exist at such time as a thermal equilibrium was achieved.

Cell pressure was monitored from consideration of the cell pressure transducer output. This provision was made to include the option of cell pressure as a fixed system parameter, and for future evaluation of predictions of cell parameters by the correlations employed to calculate vapor phase densities. Monitoring the system pressure also ensured that pressure limits of the equipment were not exceeded.

With the liquid sample mixed to a known composition, the course of action leading to photographs of pendant drops at the desired temperatures began with evacuation of the cell. With the inlet stop valve closed and the discharge stop valve open, the vacuum pump was used to bring system pressure as low as possible. Typically the system pressure was decreased to less than one inch of mercury, subject to the behavior of the vacuum pump. After evacuation the discharge

stop valve was closed and the pump stopped. The liquid sample, placed in the sample charging flask, was delivered to the cylinder of the sample introduction subsystem. With the bath and cell temperatures below the normal boiling point of the sample, the inlet stop valve was opened. The pressure drop from atmospheric to the cell provided the driving force to charge the sample. Flow of liquid into the cell was continued until the liquid level was at the bottom of the vapor cell view port, at which time the inlet stop valve was closed, the charging flask removed, and the piston started into the cylinder. Since the cylinder was full of liquid on removing the charging flask, a volume of around five milliliters of the sample was available for drop formation without further addition to the cylinder. The temperature bath was then set to reach the lowest of the temperatures at which data was desired. The optical system was aligned and the camera loaded, focused, and set for proper exposure.

When the desired temperature was reached and thermal equilibrium attained, the inlet stop valve was opened. A liquid drop was formed on the capillary tip by advancing the piston into the cylinder. As the volumes of liquid in the feed line and the drop were small, thermal equilibrium within the drop was rapidly achieved. The bath circulation pump and heater were then turned off to minimize vibration and thermal currents in the bath. The drop was adjusted to a useable size and shape and allowed to become static and stable. The desired photographs of the drop were taken, with cell temperature recorded at the time of each exposure.

The size of the drop relative to the capillary diameter and the drop shape are the factors of most influence on the usefulness

of the drop for the calculation of interfacial tension. According to Stauffer (24), drops of a nearly spherical shape have the highest inherent inaccuracy. Spherical shape is the result of using a capillary whose diameter is too small for the fluid under consideration, so that the drop diameter too greatly exceeds the capillary diameter. In terms of shape factor, this situation produces unusually small values for the parameter S. In contrast, when the fluid is of a surface tension too small for the capillary chosen, the drop diameter is smaller than the capillary diameter. The shape factor, S, is then of too large a magnitude to be useful and the drop itself is highly unstable. Both of these situations are easily avoided. The capillary size can be chosen from a prediction of the order of magnitude of the interfacial tension so that the drop and capillary diameters are compatible. For the systems used, capillary tips of fifteen gauge (0.07204 inches) and seventeen gauge (0.05803 inches) covered the required range of drop sizes.

With the capillary properly sized, the remaining influence on drop shape which falls under the control of the operator is the extent to which the drop is allowed to protrude from the tip of the capillary. Niederhauser and Bartell (17) indicate that there is a minimum size for the drop to be useful. That minimum corresponds to a drop length equal to its equatorial diameter, in which case the selected plane and the end of the capillary tip would coincide. Kellizy (12) preferred the other extreme in drop length: the maximum size drop that would remain pendant. The best compromise of these extremes appeared to be toward the smaller drop. A large drop is too prone to inherent instability and internal convection currents. In Figure 1 a pendant

drop is represented. In such a drop the liquid functions somewhat as a lens, concentrating light incident upon one side of the drop to a region near the longitudinal axis on the opposite side. When the drop is longer than its equatorial diameter, the light concentrated forms two distinct regions. The separation between these two regions locates the minimum diameter of the drop, and the termination of the uppermost region occurs very near to the lower end of the capillary. From consideration of this pattern the drop to be considered was formed; rather small, but decidedly greater than the acceptable minimum. Thus the drops were reasonably stable in nature but did not approach the minimum to the point where they might possibly contain a portion of the capillary tip.

With several photographs of drops having been obtained at the initial temperature setting, the inlet stop valve was closed. The bath control was set for the next temperature level and the procedure was continued over the temperature range of concern.

As the temperature of the system was increased from one level to the next, some care had to be exercised to avoid exceeding the pressure limitations of the vapor cell. An increase in specific volume of the liquid sample was associated with the temperature rise. The tendency was for the vapor cell to completely fill with liquid, at which point any further temperature rise would produce an excessive pressure increase. The system reacted by moving the quartz windows to compress the teflon washers. Liquid then flowed around the unseated o-rings to escape through the viewports of the vapor cell. Thus further liquid expansion did not increase the cell pressure to the point of equipment failure, but the vapor cell window installations had to be reseated,

interrupting the run. To avoid this problem, liquid sample was periodically discharged from the cell. The discharge stop valve was opened for long enough to allow the liquid level to return to the bottom of the vapor cell windows.

The photographs obtained were projected on the Vanguard CD-11 motion analyzer. The capillary, equatorial, and selected plane diameters were measured for each drop.

CHAPTER V

EXPERIMENTAL RESULTS

The systems for which experimental data were obtained were binary mixtures of normal-pentane in para-xylene and acetone in water, of various compositions. The temperature range over which these systems were considered was 125°F. to 400°F. System pressure was the saturation pressure of the particular mixture at the given temperature.

The values of interfacial tension are for the binary liquid drops in an environment of their corresponding equilibrium vapor. These values are those arrived at through application of equation (2) to values of a shape dependent parameter, (d_e^2/H), which was computed from the appropriate dimensions of each drop photographed. Values of liquid density are predictions of a modified Rackett equation (20) by Deam, Kellizy and Maddox (5) (13), which had been fitted to the specific mixtures of concern. Vapor phase densities for the pentane-xylene mixtures were predicted from the Redlich-Kwong equation of state as approached through the N.G.P.A. K&H program (6). Vapor phase densities for the acetone-water mixtures are the result of calculations based on compressibility factor tables from Lyderson, Greenkorn and Hougen (14). The interfacial tension values for pure water are predicted from the correlation of Hakim, Steinberg, and Stiel (8), which is given along with the values predicted in Appendix C.

Tables IX through XII of Appendix D give results for four compositions of normal-pentane in para-xylene. Table I gives arithmetic mean values of interfacial tension for these mixtures at arithmetic mean temperature points. Figure 8 is a plot of these mean values, interfacial tension as a function of temperature for lines of constant composition. Figure 9 is a cross plot of this information to give interfacial tension as a function of composition for lines of constant temperature.

Tables XIII through XV of Appendix D give results for three compositions of acetone in water and Table VIII in Appendix C gives the results of calculations to predict similar information for pure water. Table II gives arithmetic mean values of interfacial tension for the mixtures in Tables XIII through XV at arithmetic mean temperature points. Figure 10 is a plot of these mean values and the values of Table VIII for pure water, interfacial tension as a function of temperature for lines of constant composition. Figure 11 is a cross plot from Figure 10 to give interfacial tension as a function of composition for lines of constant temperature.

TABLE I

ARITHMETIC MEAN INTERFACIAL TENSIONS FOR
THE NORMAL-PENTANE AND PARA-XYLENE
BINARY SYSTEMS

Composition Mole % N-Pentane	Mean Temp. Degrees F.	Mean γ Dynes/cm.
0	148.6	22.24
	205.0	19.81
	254.5	17.18
	301.1	14.53
	349.9	12.21
	394.5	9.79
10.3	150.0	21.01
	203.6	17.76
	254.9	15.06
	300.1	12.81
	350.7	10.53
	392.7	8.41
90.0	148.7	12.32
	205.3	9.09
	230.5	7.48
	256.5	6.26
99+	150.0	11.55
	175.5	10.07
	201.5	8.53
	227.4	6.88
	250.8	5.57
	274.0	4.37
	302.4	3.17

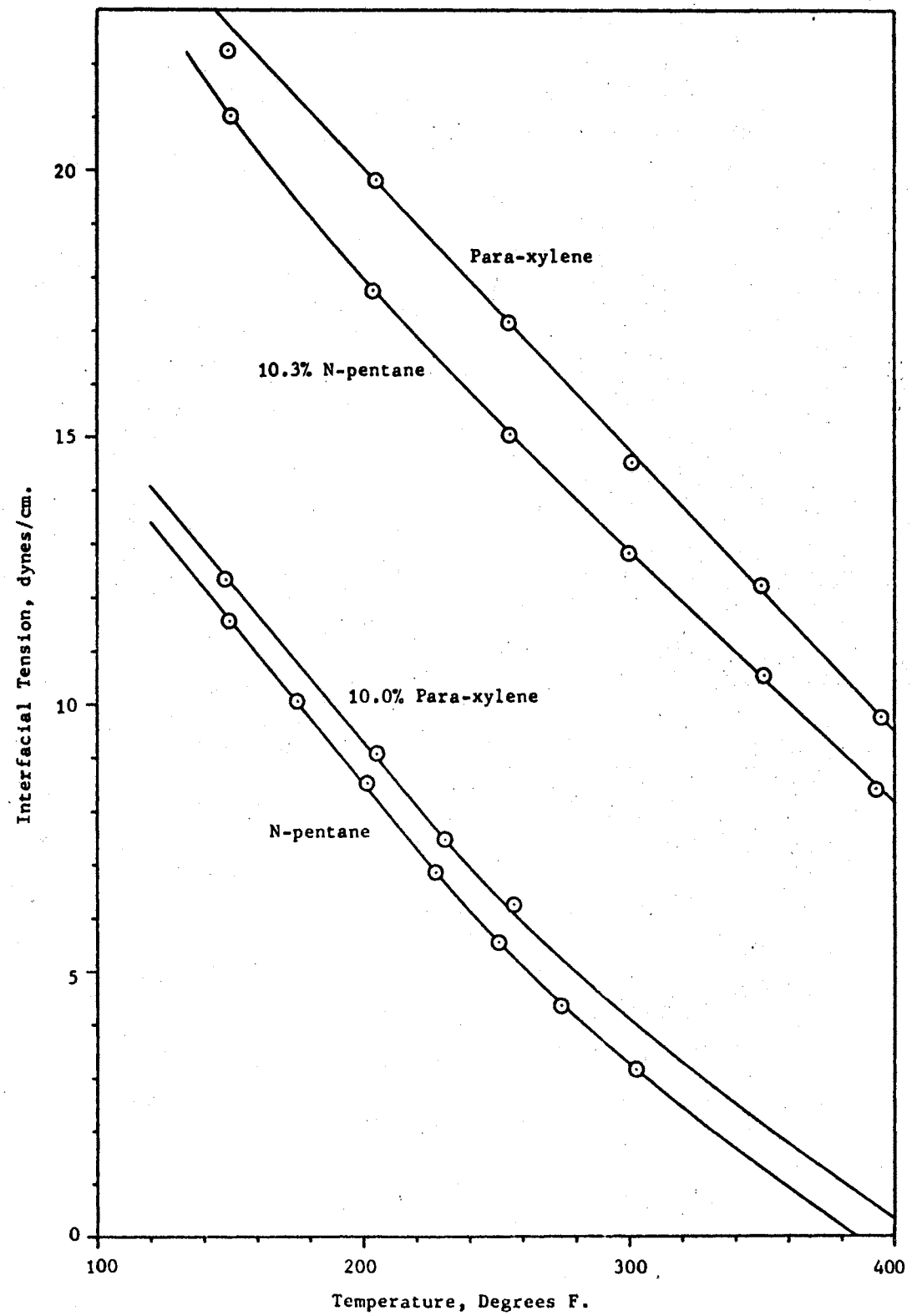

Figure 8. The Interfacial Tension of Mixtures of Normal-pentane and Para-xylene, as a Function of Temperature

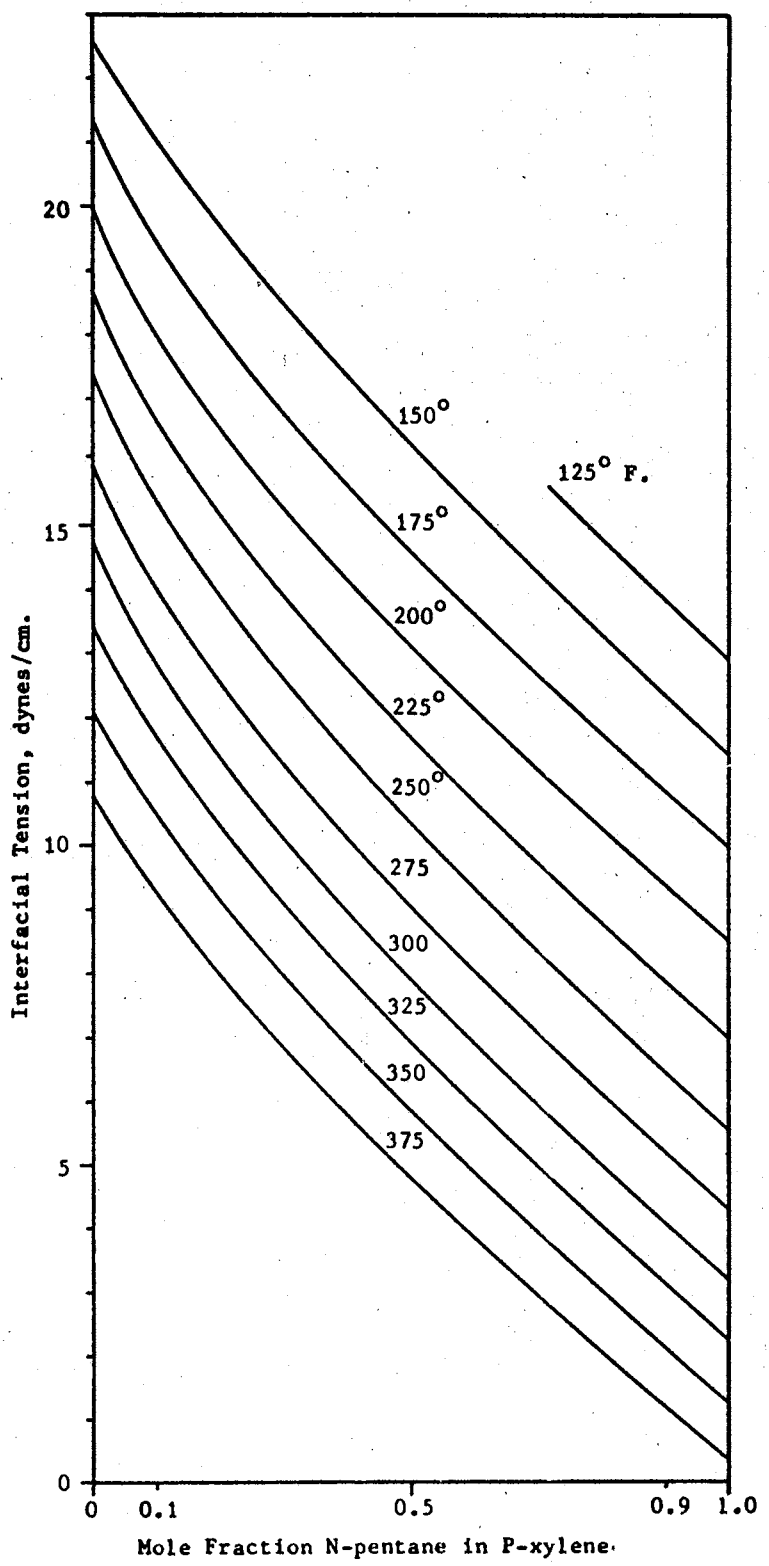

Figure 9. The Interfacial Tension of Mixtures of Normal-pentane and Para-xylene, as a Function of Composition

TABLE II

ARITHMETIC MEAN INTERFACIAL TENSIONS FOR
THE ACETONE AND WATER
BINARY SYSTEMS

Composition Mole % Acetone	Mean Temp. Degrees F.	Mean γ Dynes/cm.
30.0	151.9	23.12
	202.9	20.26
	252.7	16.50
	256.7	16.99
	304.0	13.66
	355.1	11.01
	379.6	9.73
70.0	154.1	19.02
	203.3	15.85
	252.1	12.76
	303.6	9.65
	330.3	7.99
	358.1	6.37
	383.8	4.83
100.	149.0	17.62
	204.1	13.71
	258.6	9.95
	303.1	7.38
	308.5	7.09
	329.7	5.87
	334.0	5.64
	357.7	4.41
	382.4	2.96

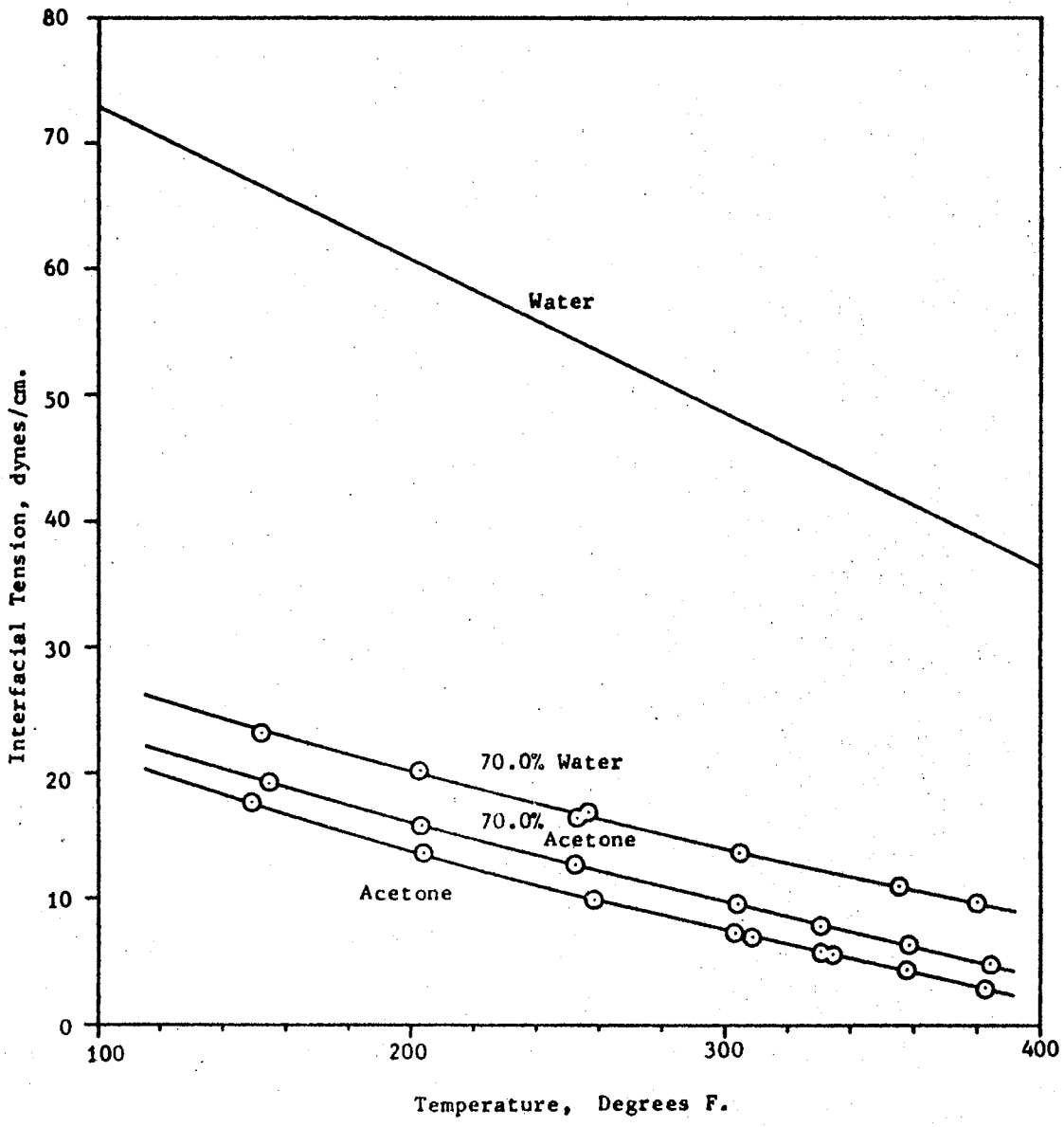

Figure 10. The Interfacial Tension of Mixtures of Acetone and Water, as a Function of Temperature

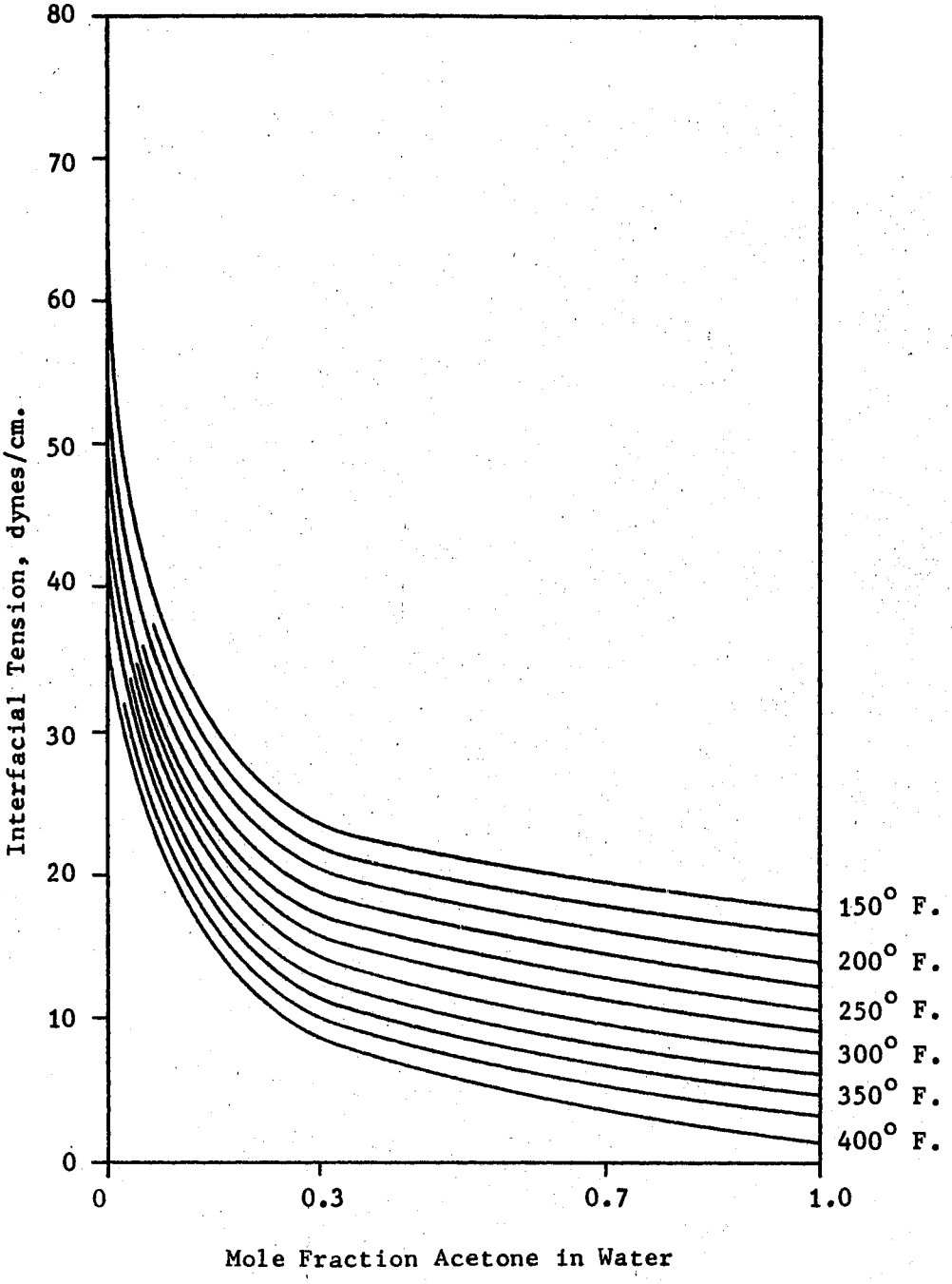

Figure 11. The Interfacial Tension of Mixtures of Acetone and Water, as a Function of Composition

CHAPTER VI

DISCUSSION OF RESULTS

Experimental data obtained for the pure components were compared to information available in the literature. The comparison was necessarily qualitative in nature since this work dealt exclusively with liquids in contact with their equilibrium vapor phases at elevated temperature and pressure conditions. Data available from previous work generally have been arrived at from consideration of the liquid in contact with air at atmospheric pressure and at temperatures below the normal boiling point. The interfacial tension was not expected to be identical for a liquid in contact with different vapors or gases, but the magnitude of the difference was expected to be small enough that the comparison of data would remain useful as an indication that the data obtained experimentally were of a reasonable magnitude.

The limiting accuracy of the method by which the data were obtained is shown in Appendix E to be in the range of $\pm$ 2%. This figure was arrived at through consideration of the best accuracy to be expected in the measurement of the system parameters and the effect of these on the most probable error in the interfacial tension predicted from such parameters.

Normal-Pentane Experimental Results

The arithmetic mean values of data taken for normal-pentane, as presented in Table I, were graphically compared to data of Rossini et al. (23). The results of the comparison are seen in Figure 12. The data of this work were reasonable compatible with those of Rossini, considering the differences in the systems considered. The data obtained experimentally exhibited an average absolute deviation of 1.11 per cent from the mean values presented. Generally a higher deviation occurred in the data obtained using a fifteen guage capillary than in that obtained using a seventeen guage tip. This was attributed to the use of the fifteen guage tip for small drops and low interfacial tensions near the limits of usefulness for that tip size. The curve of interfacial tension as a function of temperature presented in Figure 8 was extended beyond the highest temperature for which data were taken for normal-pentane by assigning an interfacial tension of zero to a temperature of 386°F., the critical temperature of pure normal-pentane.

Para-Xylene Experimental Results

The arithmetic mean values of interfacial tension for para-xylene are presented in Table I. These values were graphically compared to data of Rossini et al., and this comparison is presented in Figure 12. Agreement between the curves of experimental data and that of Rossini was quite good. The experimental data points exhibited an average absolute deviation of 0.94 per cent from the mean values presented. The mean data point located at an average temperature of 148.6°F. was judged to have indicated too low a value for interfacial tension. In locating the curve of Figure 8, this data point was ignored and the

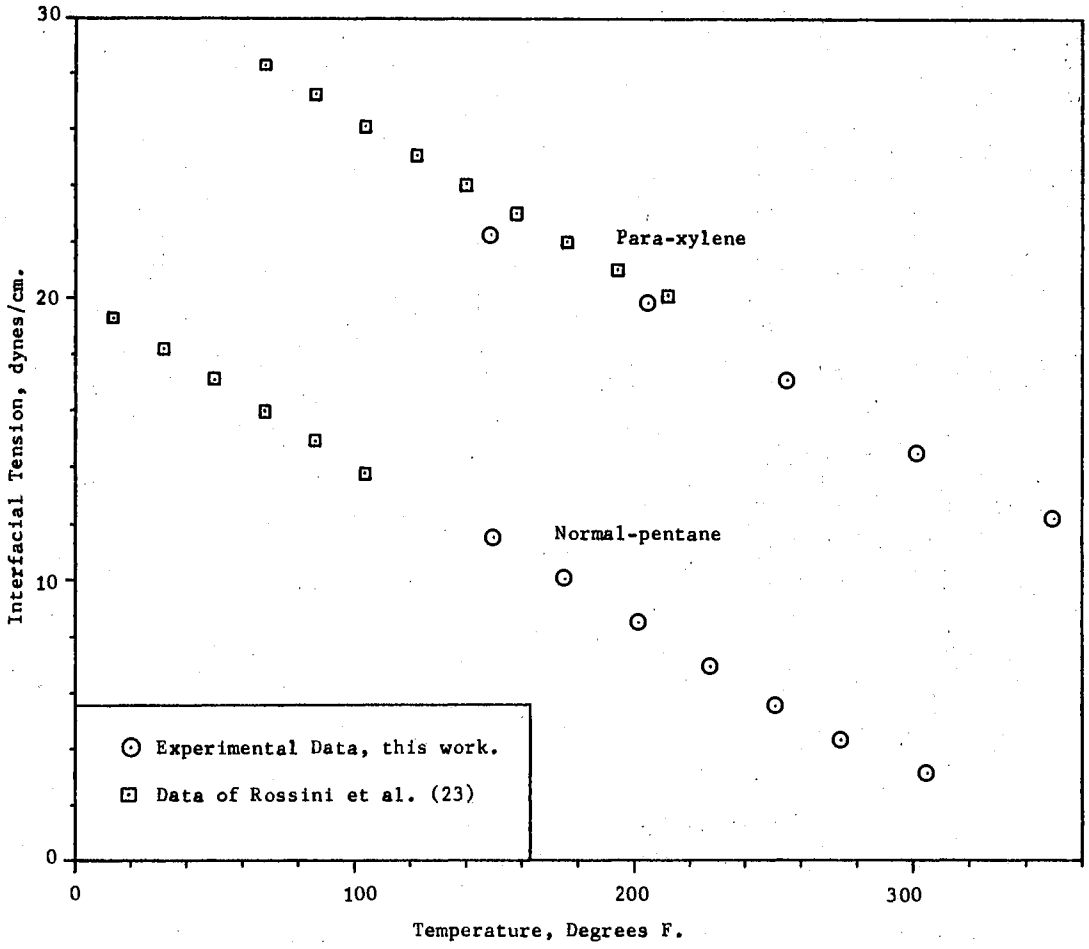

Figure 12. Comparison of Experimental Interfacial Tension of Pure Normal-pentane and Para-xylene to Data from Previous Works

curve was determined by the remaining points. The data of Rossini et al. tend to support this decision through exceptional agreement with the curve of the remaining points. The single data point in question is lower than the value predicted by the curve selected by 0.54 dynes per centimeter, or 2.37 per cent of the predicted value.

Acetone Experimental Results

The arithmetic mean values of interfacial tension for acetone are presented in Table II. These values were compared to data from the International Critical Tables (16). The comparison is presented in Figure 13. Experimental data were in extremely close agreement with those of the literature source. The experimental data points exhibited an average absolute deviation of 0.84 per cent from the mean values presented.

Mixtures of Normal-Pentane and Para-xylene

The data for 10.3 mole per cent normal-pentane showed an average absolute deviation of 1.11 per cent from the mean values presented in Table I. The data for 90.0 mole per cent normal-pentane showed such an average deviation of 0.66 per cent. Extension of the curve for 90.0 mole per cent normal-pentane to temperatures beyond those for which data were taken was accomplished by assigning the value of zero to the interfacial tension at a temperature of 409°F. This corresponds to the critical temperature predicted for the mixture by the modified Rackett program (5). Between this temperature and the highest temperature for which data were taken, the curve was assigned a shape compatible with the trend set by the curve for normal-pentane.

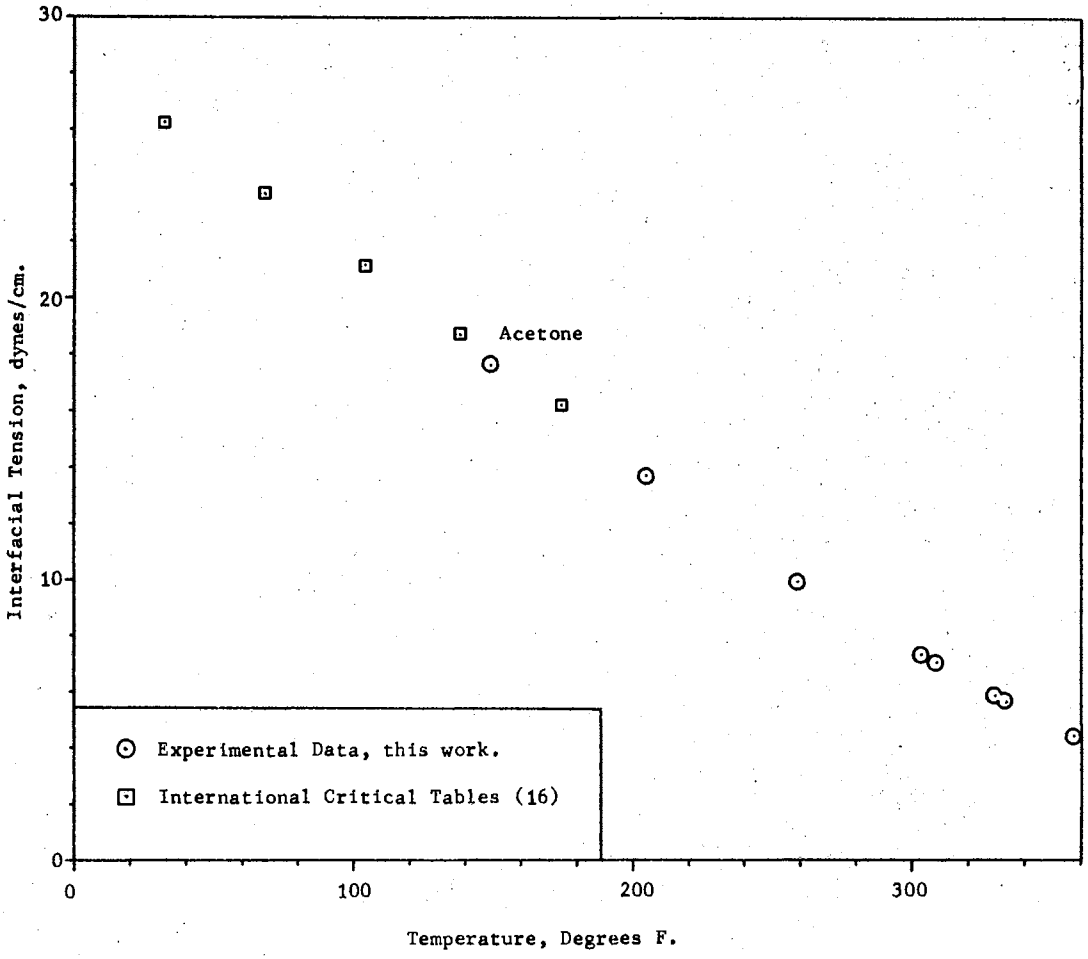

Figure 13. Comparison of Experimental Interfacial Tension of Pure Acetone to Data from Previous Works

The curves of Figure 8 were plotted as interfacial tension as a function of temperature for the four compositions considered. From these curves, those of Figure 9 were taken as interfacial tension as a function of composition for lines of constant temperature. The curves of Figure 9 exhibited a greater change of interfacial tension for a composition change near the component of highest interfacial tension, para-xylene. This non-linear behavior is generally to be expected of mixtures. This characteristic and the general uniformity of the curves of Figure 9 indicate that the curves in Figure 8 are of a reasonable nature.

Mixtures of Acetone and Water

The data for 30.0 mole per cent acetone exhibited an average absolute deviation of 1.04 per cent from the mean values presented in Table II. The data for 70.0 mole per cent acetone showed a similar deviation of 1.09 per cent. The curves representing the mean data points of Table II are presented in Figure 10. The curves were plotted as interfacial tension as a function of temperature for the compositions considered. A similar curve for water was predicted from the correlation of Hakim, Steinberg and Stiel (8), as presented in Appendix C. From the curves of Figure 10, those of Figure 11 were taken as interfacial tension as a function of composition for lines of constant temperature. These curves exhibit a greater change in the interfacial tension for a composition change near the component of higher interfacial tension, water. The curves compare well in shape to similar curves for acetone and water mixtures presented by Howard and McAllister (10). The data from that source were taken against air

and at temperatures below the normal boiling points of the mixtures considered. Curves from that work representing mixtures at 20° and 50° C. are presented, along with the curves of Figure 11, in Figure 14.

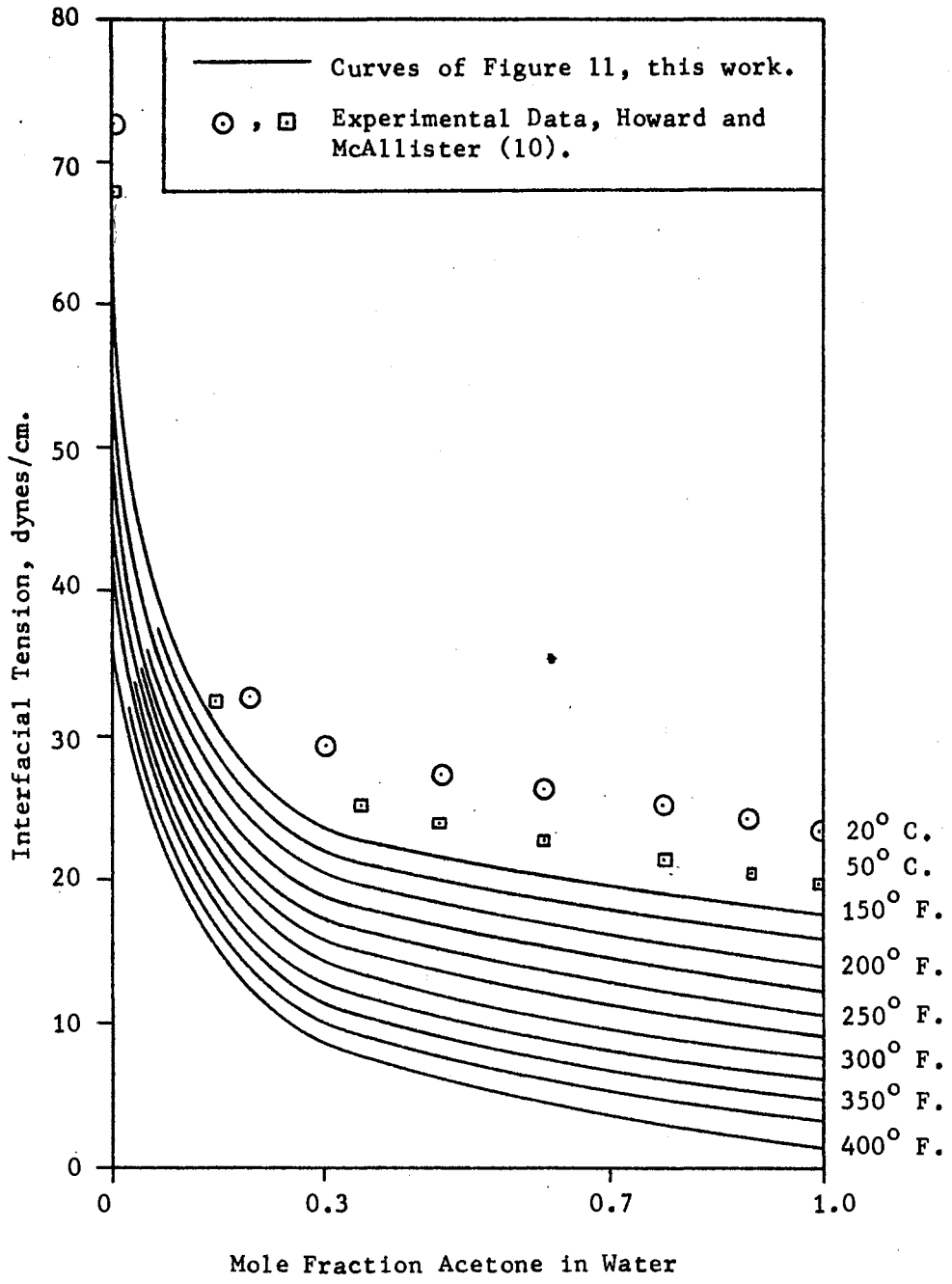

Figure 14. Comparison of Experimental Interfacial Tension of Water-Acetone Mixtures to Data from Previous Works

CHAPTER VII

THE ACCURACY OF PREDICTIVE METHODS

The adequacy of the information that was experimentally obtained for the interfacial tension of the systems considered was illustrated in the preceding chapter, through comparison of the experimental results of this study with similar results from previous works. Predictions of interfacial tension for the systems of concern were then to be obtained through the correlations of various authors. These predictions were to be compared to the experimental data to determine the ability of the correlations to reflect the physical behavior of the systems considered.

The predictive methods of Sugden (25), Reilly and Rae (22), and Brock and Bird (3) were used to consider the systems of pure polar fluids. Mixtures of non-polar materials were considered through the correlation of Weinaug and Katz (27). Mixtures of polar substances were considered through the correlation of Tamura et al. (26). Each of these methods was described in Chapter II.

Values for the parachor of the substances considered were selected from the work of Quayle (19) or computed from the equation of Reilly and Rae (22), as appropriate. Liquid phase densities were evaluated through the modified Rackett program (5). Vapor phase densities, phase compositons and molecular weights were obtained through the N.G.P.A. K&H program (6). Critical constants were taken from A.P.I. Research

Project 44 (1) and the International Critical Tables (16). Values of the Reidel critical parameter (21) were obtained through the approach described in Pitzer et al. (18).

The predictions of the correlations used to consider pure non-polar fluids are presented, along with the corresponding experimental mean data points, in Table III for normal-pentane and Table IV for para-xylene. The predictions of the equation of Sugden exhibited an average absolute deviation from the experimental mean data points of 15.05 per cent for normal-pentane and 2.24 per cent for para-xylene. The correlation of Reilly and Rae showed such deviations of 9.59 per cent for normal-pentane and 1.66 per cent for para-xylene, and the predictions of the Brock and Bird approach exhibited deviations of 2.42 per cent for normal-pentane and 4.36 per cent for para-xylene. Table V presents the predictions of the correlation of Hakim et al. and the corresponding mean data points for acetone. This approach exhibited an average absolute deviation of 6.28 per cent from the experimental mean data points in its prediction of the behavior of acetone.

The predictions of the interfacial tension for mixtures of normal-pentane and para-xylene, obtained from the Weinaug and Katz correlation, are presented in Table VI along with the corresponding mean data points. These predictions exhibited an average absolute deviation of 4.34 per cent from the mean data points presented for the mixture of 10.3 mole per cent normal-pentane. A similar deviation of 17.88 per cent was shown for the mixture of 90.0 mole per cent normal-pentane.

Values of the interfacial tension of binary mixtures of acetone and water were predicted by the correlation of Tamura et al. (26).

TABLE III

PREDICTED INTERFACIAL TENSION
OF NORMAL-PENTANE

Temp. Degrees F.	Mean Data	Sugden (Quayle)	Reilly & Rae	Brock & Bird
150.0	11.55	13.21	12.53	11.11
175.5	10.07	11.47	10.89	9.66
201.5	8.53	9.75	9.25	8.22
227.4	6.88	8.07	7.66	6.83
250.8	5.57	6.60	6.27	5.62
274.0	4.37	5.19	4.93	4.47
302.4	3.17	3.56	3.34	3.12

TABLE IV

PREDICTED INTERFACIAL TENSION
OF PARA-XYLENE

Temp. Degrees F.	Mean Data	Sugden (Quayle)	Reilly & Rae	Brock & Bird
148.6	22.24	23.17	22.35	23.57
205.0	19.81	19.99	19.28	20.39
254.5	17.18	17.30	16.68	17.67
301.1	14.53	14.86	14.33	15.18
349.9	12.21	12.38	11.94	12.65
394.5	9.79	10.18	9.81	10.41

TABLE V

PREDICTED INTERFACIAL TENSION
OF ACETONE

Temp. Degrees F.	Interfacial Tension in dynes/cm. Mean Data	Hakim et al.
149.0	17.62	16.97
204.1	13.71	13.61
258.6	9.95	10.36
303.1	7.38	7.78
308.5	7.09	7.48
329.7	5.87	6.28
334.0	5.64	6.04
357.7	4.41	4.74
382.4	2.96	3.42

TABLE VI

INTERFACIAL TENSION OF MIXTURES OF
NORMAL-PENTANE AND PARA-XYLENE

Mole % N-pentane	Temp. Degrees F.	Interfacial Tension in dynes/cm.	
		Mean Data	Weinaug & Katz
10.3	150.0	21.01	21.72
	203.6	17.76	18.66
	254.9	15.06	15.85
	300.1	12.81	13.44
	350.7	10.53	10.85
	392.7	8.41	8.78
90.0	148.7	12.32	14.38
	205.3	9.09	10.60
	230.5	7.48	9.00
	256.5	6.26	7.38

This method used the values of density and interfacial tension for the pure components to predict the interfacial tension of the mixture at the same temperature. The pure component densities were obtained from the modified Rackett program (5) and the values of interfacial tension for the components from the correlation of Hakim et al. (8). The error in prediction of the pure component properties, in particular those for acetone, was then to be expected to influence the error associated with the predictions for the mixtures. The predictions for mixtures of 30.0 and 70.0 mole per cent acetone are presented, along with the corresponding mean data values, in Table VII. These predictions exhibited an average absolute deviation from the mean data values of 15.9 per cent for the mixture of 30.0 mole per cent acetone and 11.8 per cent for that of 70.0 mole per cent acetone. The deviation from the mean data became noticeably larger with increasing temperature. This effect was thought to be due to an assumption made in deriving the correlation. Tamura chose to define the parachor as a function of liquid density rather than the phase density difference, and to neglect the vapor density contribution. For an increase in temperature the liquid density would decrease and the vapor pressure of the system would increase, forcing the vapor density to increase. Thus at higher temperatures the vapor density contribution would be of more influence and the fact that Tamura chose to neglect that contribution was reflected in larger errors in the predictions of his correlation.

TABLE VII

INTERFACIAL TENSION OF MIXTURES
OF ACETONE AND WATER

Mole % Acetone	Temp. Degrees F.	Interfacial Tension in dynes/cm.	
		Mean Data	Tamura et al.
30.0	151.9	23.12	21.62
	202.9	20.26	18.39
	252.7	16.50	15.14
	256.7	16.99	14.87
	304.0	13.66	11.68
	355.1	11.01	8.14
	379.6	9.73	6.38
70.0	154.1	19.02	17.70
	203.3	15.85	14.66
	252.1	12.76	11.67
	303.6	9.65	8.57
	330.3	7.99	6.99
	358.1	6.37	5.36
	383.8	4.83	3.87

CHAPTER VIII

CONCLUSIONS AND RECOMMENDATIONS

Conclusions

The purpose of the study, as stated in the introduction, was to produce an apparatus through which the interfacial tension of a system could be accurately evaluated over a wide range of conditions. The apparatus was then to be used to investigate systems of immediate concern.

An apparatus was constructed to evaluate interfacial tension of multicomponent systems to an accuracy of within two or three per cent. The range of temperature over which operation was feasible was from 150°F. to 400°F. and the system pressure was limited to below 1000 psig. The apparatus was designed to limit changes in liquid phase composition to below 0.1 mole per cent over an excursion through the useful temperature range. The temperature was measurable to within 0.1°F. and the pressure to within 2 psig.

The apparatus was used to investigate binary systems of normal-pentane in para-xylene and acetone in water. Experimental data obtained for pure components normal-pentane, para-xylene, and acetone, and for mixtures of acetone in water were compatible with similar data from various literature sources.

Predictions of interfacial tension by several correlations were compared to corresponding values from the experimental data. Average

absolute deviations of the predicted values from the data, over the temperature range for which data were taken, ranged from 1.7 per cent to 17.9 per cent. Generally, the correlations considered were not to be trusted for less than ten per cent deviation in their predictions, and were increasingly unreliable at higher temperatures.

Recommendations

The ability to obtain accurate information on interfacial tension from the apparatus seemed most dependent upon two aspects of equipment configuration. Good drop control is essential since the pendant drop procedure depends upon the analysis of a static drop. If the drop considered was, in fact, of a dynamic nature, the mathematical analysis employed would be invalid. A method of sample introduction and drop control is suggested to provide the desired operator control over the flow of liquid to and from the drop. The method would require replacement of the sample introduction subsystem by a mercury driven charging system controlled through a micrometer needle valve, as shown in Figure 15. Complete shielding from the temperature bath fluid is recommended for the liquid feed line to avoid the effects of temperature cycling on the fluid in the line. The suggested alteration should provide excellent drop control and make the use of the apparatus feasible for highly volatile materials.

The optical equipment used to obtain photographs of the liquid drops is a primary factor in determining the accuracy of the data obtained. A recent article by Hyzer (11) described the problems associated with drop photography. The author suggested the use of a constant wavelength laser for the light source, and that an optical

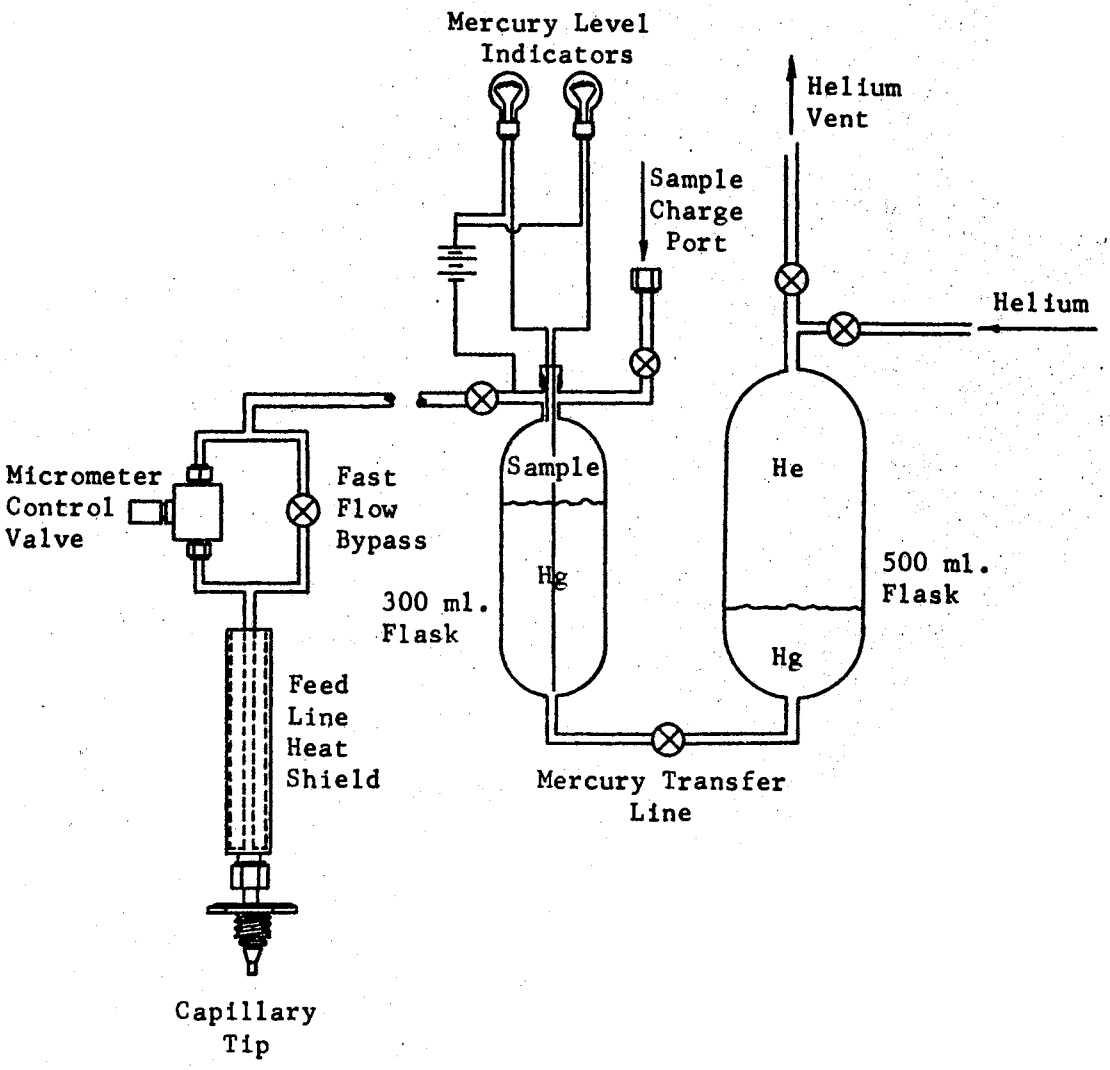

Figure 15. Mercury Driven Charging System

bench be used to guarantee precise alignment. The addition of a system similar to that recommended by Hyzer would improve upon the accuracy available. A bench designed to fix the location and alignment of the optical equipment relative to the vapor cell viewports is recommended.

Of the two suggested alterations, the addition of the sample introduction and drop control equipment would be the most advantageous. The precise control over drop size and the guarantee that the drop is static are required to ensure that the method is valid. The precision optical equipment would facilitate the evaluation of drop parameters and eliminate image distortions, but is not critical to the validity of the approach.

A SELECTED BIBLIOGRAPHY

(1) Am. Petr. Inst. Res. Proj. 44. "Selected Values of Thermodynamic Properties of Hydrocarbons and Related Compounds." Texas A. & M., College Station, Texas, 1963.

(2) Andreas, J. M., E. A. Hauser, and W. B. Tucker, "Boundary Tension by Pendant Drops." Journal of Physical Chemistry 43. 1001 (1938).

(3) Brock, J. R., and R. B. Bird. "Surface Tension and the Principle of Corresponding States." A. I. Ch. E. Journal 1. 174 (1955).

(4) Deam, J. R. "Interfacial Tension in Hydrocarbon Systems." (Unpub. Ph.D. thesis, Oklahoma State University, 1969).

(5) Deam, J. R., I. K. Kellizy, and R. N. Maddox. "Calculating Density of Saturated Hydrocarbon Mixtures." Proceedings of the Forty-Eighth Annual Convention. N. G. P. A., 48 (1969).

(6) Erbar, J. H. "K & H Computer Program, I. B. M. Series 360." N. G. P. A. (1966).

(7) Fordham, S. "On the Calculation of Surface Tension from Measurements of Pendant Drops." Proceedings of Royal Society (London), vol. 194A, 1 (1948).

(8) Hakim, D. I., D. Steinberg, and L. I. Stiel. "Generalized Relationship for the Surface Tension of Polar Fluids." Ind. Eng. Chem. Fundam. vol. 10, no. 1, 174 (1971).

(9) Hough, E. W., B. B. Wood, and M. J. Rzasa. "Adsorption at Water-Helium, - Methane and - Nitrogen Interfaces at Pressures to 15,000 p.s.i.a." Journal of Physical Chemistry 56. 996 (1952).

(10) Howard, S. H., and R. A. McAllister. "Surface Tension of Acetone - Water Solutions up to their Normal Boiling Points." A. I. Ch. E. Journal 3. 325 (1957).

(11) Hyzer, W. G. "Photographic Recording of Liquid Drops." Research/Development. 42, Dec. (1971).

(12) Kellizy, I. K. "Surface Tension in Hydrocarbon and Related Systems." (Unpub. M.S. thesis, Oklahoma State University, (1970).

(13) Killgore, C. A., V. K. Mathur, J. H. Erbar, and R. N. Maddox. "Calculating Density of Saturated Hydrocarbon Mixtures." (Paper presented at 68th Nat'l. Meeting, A. I. Ch. E., 6th Petrochemical and Refining Exposition, Houston, Texas, 1971).

(14) Lyderson, A. L., R. A. Greenkorn, and O. A. Hougen. "Generalized Thermodynamic Properties of Pure Fluids." University of Wisconsin, 1955.

(15) Mills, O. S. "Tables for use in the Measurement of Interfacial Tensions Between Liquids with Small Density Differences." British Journal of Applied Physics 4. 247 (1953).

(16) National Research Council of the United States of America. International Critical Tables of Numerical Data, Physics, Chemistry and Technology. New York: McGraw-Hill, 1928.

(17) Niederhauser, D. O., and F. E. Bartell. "A Corrected Table for the Calculation of Boundary Tensions by the Pendant Drop Method." Report of Progress -- Fundamental Research on Occurrence and Recovery of Petroleum. A. P. I., Baltimore, Md., 114 (1950).

(18) Pitzer, K. S., D. Z. Lippmann, R. F. Curl, Jr., C. M. Huggins, and D. E. Petersen. "The Volumetric and Thermodynamic Properties of Fluids." J. Am. Chem. Soc. 77. 3433 (1955).

(19) Quayle, O. R. "The Parachors of Organic Compounds." Chemical Reviews 53. 439 (1953).

(20) Rackett, H. G. "Equations of State for Saturated Liquids." Journal of Chemical and Engineering Data, vol. 15, 514, (1970).

(21) Reidel, L. "Eine neue Universelle Dampfdruckformel." Chem. Ing. Tech. 26. 83 (1954).

(22) Reilly, J. and W. N. Rae. Physico - Chemical Methods. 3rd ed., Princeton, N. J.: D. Van Nostrand, (1939).

(23) Rossini, F. D., K. S. Pitzer, R. L. Arnett, R. M. Braum, and G. C. Pimentel. Selected Values of Physical and Thermodynamic Properties of Hydrocarbons and Related Compounds. Pittsburgh, Pennsylvania: Carnegie Press, 1953.

(24). Stauffer, C. E. "The Measurement of Surface Tension by the Pendant Drop Technique." Journal of Physical Chemistry 69. 1933 (1965).

(25) Sugden, S. The Parachor and Valency. London: George Ruthledge and Sons, Ltd., 1930.

(26) Tamura, M., M. Kurata, and H. Odani. "Practical Method for Estimating Surface Tensions of Solutions." Bulletin of the Chem. Soc. of Japan 28. 83 (1955).

(27) Weinaug, C. F., and D. L. Katz. "Surface Tension of Methane - Propane Mixtures." Ind. and Eng. Chem. 35. 239 (1943).

APPENDIX A

LIQUID FLASK VOLUME

LIQUID FLASK VOLUME

The purpose of the liquid chamber of the cell was to contain a volume of liquid sample sufficient to provide fourteen cubic centimeters of equilibrium vapor without appreciably changing in composition over the course of a run. The flask was five hundred cubic centimeters in volume. Calculations were made to show the change in liquid phase composition associated with the formation of the required equilibrium vapor at temperatures near the extremes of the range to be encountered during an experimental run. The binary system of normal-pentane in para-xylene was chosen for consideration and a liquid phase composition of 10.32 mole per cent normal-pentane was assigned.

Liquid composition:	10.32 mole % n-pentane 89.68 mole % p-xylene
Temperature:	150.0°F.

From the N.G.P.A. K&H program, a bubble point calculation predicted values for the following system parameters:

Pressure:	6.62 psia
Vapor density:	0.00128 gm./c.c.
Vapor composition:	79.67 mole % n-pentane 20.33 mole % p-xylene
Mole weight (vapor):	79.07 gms./gm. mole
Mole weight (liquid):	102.66 gms./gm. mole

From the modified Rackett program, the liquid density was computed to be 0.79756 gm./c.c.

Liquid sample charged:

500 c.c.(0.79756 gm./c.c.) = 398.78 grams of liquid.

398.78 gm./(102.66 gm./mole) = 3.8845 moles of liquid.

0.1032(3.8845 moles) = 0.4009 moles of n-pentane.

0.8968(3.8845 moles) = 3.4836 moles of p-xylene.

Vapor formed:

14 c.c.(0.00128 gm./c.c.) = 0.01792 grams of vapor.

0.01792 gm./(79.07 gm./mole) = 0.00023 moles of vapor.

0.7967(0.00023 moles) = 0.00018 moles of n-pentane.

0.2033(0.00023 moles) = 0.000046 moles of p-xylene.

Liquid remaining:

(0.4009-0.00018) moles = 0.4007 moles of n-pentane.

(3.4836-0.0000) moles = 3.4836 moles of p-xylene.

So the liquid composition has become 10.315 mole per cent normal-pentane and 89.685 mole per cent para-xylene. The change in liquid composition is on the order of 0.005 mole per cent.

Liquid composition:	10.32 mole % n-pentane 89.68 mole % p-xylene
Temperature:	393°F.

From the N.G.P.A. K&H program, a bubble point calculation predicted values for the following system parameters:

Pressure:	104.4 psia
Vapor density:	0.01894 gm./c.c.
Vapor composition:	46.17 mole % n-pentane 53.83 mole % p-xylene
Mole weight (vapor):	90.46 gms./gm. mole
Mole weight (liquid):	102.66 gms./gm. mole

From the modified Rackett program, the liquid density was computed to be 0.65439 gm./c.c.

Liquid sample charged:

500 c.c.(0.65439 gm./c.c.) = 327.195 grams of liquid.

327.195 gm./(102.66 gm./mole) = 3.18717 moles of liquid.

0.1032(3.18717 moles) = 0.32892 moles of n-pentane.

0.8968(3.18717 moles) = 2.85825 moles of p-xylene.

Vapor formed:

14 c.c.(0.01894 gm./c.c.) = 0.26516 grams of vapor.

0.26516 gm./(90.46 gm./mole) = 0.002931 moles of vapor.

0.4617(0.002931 moles) = 0.001353 moles of n-pentane.

0.5353(0.002931 moles) = 0.001578 moles of p-xylene.

Liquid remaining:

(0.32892-0.00293) moles = 0.32599 moles of n-pentane.

(2.85825-0.00158) moles = 2.85667 moles of p-xylene.

So the liquid composition has become 10.242 mole per cent normal-pentane and 89.758 mole per cent para-xylene. The change in liquid composition is on the order of 0.078 mole per cent.

The assumption of constant liquid phase composition was made on the basis of the results of these calculations. In order to check the validity of such an assumption, the refractive index of the liquid phase was checked at various stages of the experimental runs for samples of 10.3 and 90.0 mole per cent n-pentane in para-xylene. A sample of the liquid phase was withdrawn from the system and its refractive index compared to a curve of index of refraction at 12.5° C. as a function of composition. The curves had been developed from

the indices of refraction of several small samples that were prepared gravimetrically on a Mettler model B-6 balance.

Sample, by weight: 384.96 grams of para-xylene
30.59 grams of n-pentane

At 12.5°C., relative to N_d = 1.4992 for para-xylene,

Sample N_d = 1.4862

This N_d corresponds to a sample composition of 10.32 mole per cent n-pentane.

The sample was charged to the cell and the experimental run initiated. Data were compiled for temperatures of 150, 200, 250, 300, and 350°F. A sample was then withdrawn for analysis. At 12.5°C., the refractive index of the sample was 1.4862. Additional data were obtained at 350 and 400°F. The run was terminated and the cell temperature returned to 120°F. An additional sample was withdrawn from the cell. Again the refractive index of the sample was 1.4862.

Sample, by weight: 71.67 grams of para-xylene
438.07 grams of n-pentane

At 12.5°C., relative to N_d = 1.4992 for para-xylene,

Sample N_d = 1.3774

This N_d corresponds to a sample composition of 90.0 mole per cent n-pentane.

The sample was charged to the cell and the experimental run initiated. Data were compiled at temperatures of 150, 200, 225, and 250°F. A sample was then withdrawn for analysis. At 12.5°C., the refractive index of the sample was 1.3774. The cell temperature was returned to 120°F., and

an additional sample was checked. Again the refractive index of the sample was 1.3774.

As the refractive index of the liquid samples remained unchanged over the duration of the experimental runs, the liquid compositions were considered to have remained unchanged within the limits of numerical significance. The composition indicated by the sample refractive index was assigned to the sample of 10.3 mole per cent n-pentane, as the gravimetric preparation of the standard samples on the Mettler balance was judged to have been more accurate than the gravimetric preparation of the larger sample.

APPENDIX B

INSTRUMENTATION CALIBRATION CURVES

INSTRUMENTATION CALIBRATION CURVES

Calibration curves were prepared for the devices used to monitor system parameters. The bath and cell thermocouples were calibrated against three reference temperatures. The reference temperatures used were the melting point of distilled water at 32°F., the boiling point of distilled water at 210.9°F. and an atmospheric pressure of 746 mmHg, and the melting point of pure tin at 449.4°F. The transducer was calibrated against a Budenberg dead weight guage tester, number 2167. The thermocouple curves are presented in Figure 16 and the transducer curve is in Figure 17.

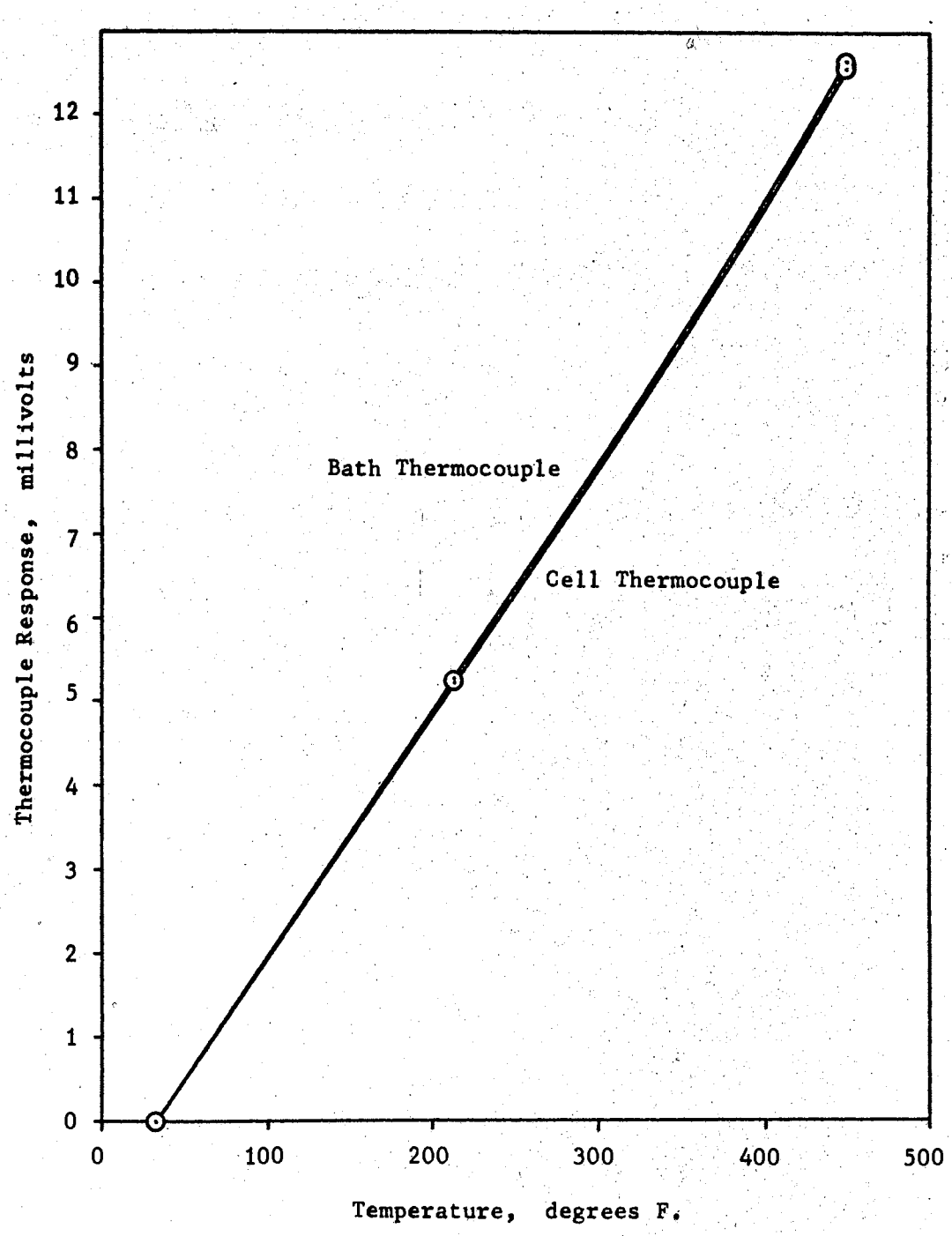

Figure 16. Thermocouple Calibration Curves

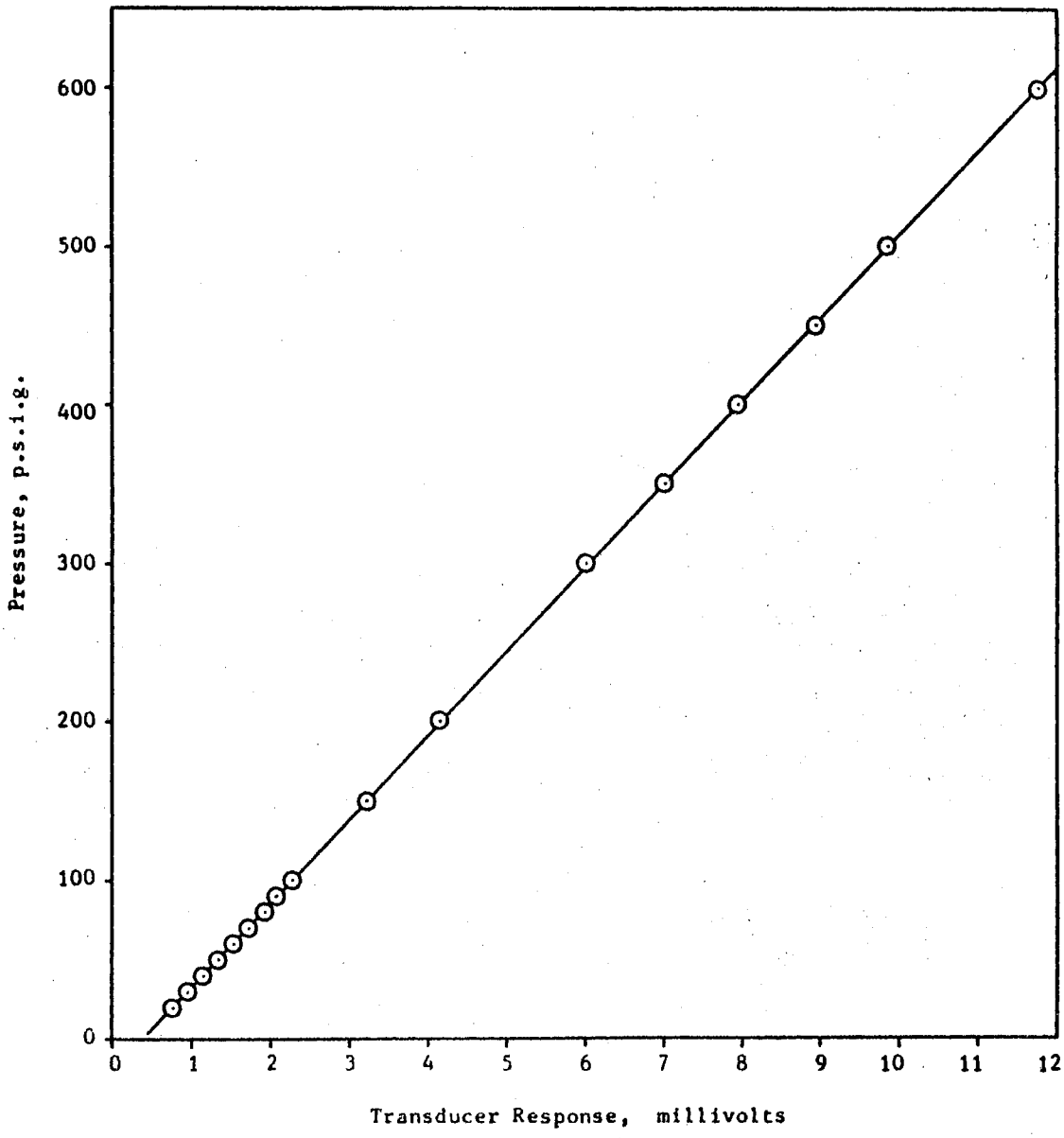

Figure 17. Transducer Calibration Curve

APPENDIX C

INTERFACIAL TENSION OF WATER

INTERFACIAL TENSION OF WATER

The attempt to obtain experimental data for the interfacial tension of pure water proved unsuccessful, primarily because of one obstacle. The high interfacial tension of water caused the liquid that condensed on the vapor cell windows to form rather large droplets. The high latent heat of vaporization for water made the droplets quite persistent, and clear photographs of the pendant drops were not obtainable.

As an alternate route to the desired information the correlation of Hakim, Steinberg and Stiel (8) suggested that the interfacial tension of polar fluids could be predicted from equation (13).

$$\gamma_R = (\gamma_R \Big| T_R = 0.6)\left(\frac{1-T_R}{0.4}\right)^{m(w,x)} \tag{13}$$

The reduced interfacial tension, γ_R, was defined by equation (14) and the function m(w,x) by equation (15). Values of w and x for water were given as 0.344 and 0.023, respectively.

$$\gamma_R = \frac{\gamma}{P_C^{2/3}\, T_C^{1/3}} \tag{14}$$

$$m(w,x) = 1.210+0.5385w-14.61x-32.07x^2-1.65w^2+22.03wx \tag{15}$$

A relationship was given to estimate the value of $(\gamma_R \Big| T_R = 0.6)$ but as data were available in this range of reduced temperature (16), a value was interpolated from the experimental information at hand.

Calculations for values of interfacial tension over the temperature range of concern were effected by this approach, and the results are provided in Table X. The interfacial tension was calculated at temperatures for which data were available, and proved to fall within the range of experimental precision claimed by the authors who supplied the data. The curve produced from this correlation was used for pure water, and appears in Figure 10.

TABLE VIII

INTERFACIAL TENSION
OF WATER

Temperature Degrees F.	Calculated γ Dynes/cm.	Experimental (16) γ Dynes/cm.
100.0	72.99	
125.0	69.91	
150.0	66.84	
175.0	63.77	
200.0	60.70	
225.0	57.64	
230.0	57.03	56.89 $\pm$ 0.2
248.0	54.82	54.89 $\pm$ 0.2
250.0	54.58	
266.0	52.62	52.84 $\pm$ 0.3
275.0	51.52	
300.0	48.47	
325.0	45.42	
350.0	42.37	
375.0	39.33	
400.0	36.30	
425.0	33.27	

APPENDIX D

EXPERIMENTAL DATA

TABLE IX

EXPERIMENTAL INTERFACIAL TENSION
FOR PARA-XYLENE

Temp. °F.	$\frac{d_e^2}{H}$	ρ_l (gm./cm.^{3})	ρ_v (gm./cm.^{3})	γ Dynes/cm.
149.0	0.02800	0.8201	0.00032	22.50
149.0	0.02829	0.8201	0.00032	22.73
148.5	0.02779	0.8204	0.00032	22.33
148.5	0.02777	0.8204	0.00032	22.32
148.5	0.02742	0.8204	0.00032	22.03
148.5	0.02733	0.8204	0.00032	21.96
148.5	0.02753	0.8204	0.00032	22.13
148.5	0.02765	0.8204	0.00032	22.22
148.5	0.02735	0.8204	0.00032	21.98
205.5	0.02524	0.7910	0.00096	19.54
205.0	0.02528	0.7913	0.00096	19.58
205.0	0.02557	0.7913	0.00096	19.80
205.0	0.02562	0.7913	0.00096	19.84
205.0	0.02556	0.7913	0.00096	19.79
205.0	0.02619	0.7913	0.00096	20.28
254.0	0.02308	0.7648	0.00224	17.25
254.0	0.02328	0.7648	0.00224	17.40
254.0	0.02369	0.7648	0.00224	17.70
255.0	0.02271	0.7642	0.00224	16.96
255.0	0.02259	0.0642	0.00224	16.87
255.0	0.02265	0.7642	0.00224	16.91
300.5	0.02009	0.7383	0.00400	14.45
300.5	0.02031	0.7383	0.00400	14.62
300.5	0.02000	0.7383	0.00400	14.39
300.5	0.02035	0.7383	0.00400	14.64
302.0	0.02016	0.7374	0.00416	14.50
302.0	0.02054	0.7374	0.00416	14.76
302.0	0.01999	0.7374	0.00416	14.36
350.0	0.01776	0.7084	0.00721	12.20
350.0	0.01781	0.7084	0.00721	12.24
350.0	0.01774	0.7084	0.00721	12.19
350.0	0.01763	0.7084	0.00721	12.12
350.0	0.01760	0.7084	0.00721	12.10
350.0	0.01774	0.7084	0.00721	12.19
350.0	0.01785	0.7084	0.00721	12.26
350.0	0.01760	0.7084	0.00721	12.10
350.0	0.01788	0.7084	0.00721	12.28
348.5	0.01811	0.7093	0.00721	12.46

TABLE IX (Continued)

Temp. °F	$\frac{d_e^2}{H}$	ρ_l (gm./cm.^{3})	ρ_v (gm./cm.^{3})	γ Dynes/cm.
395.0	0.01514	0.6791	0.0119	9.90
395.0	0.01477	0.6791	0.0119	9.66
394.5	0.01530	0.6795	0.0119	10.01
394.5	0.01462	0.6795	0.0119	9.57
395.0	0.01500	0.6791	0.0119	9.81
394.0	0.01496	0.6798	0.0117	9.80
394.0	0.01505	0.6798	0.0117	9.86
394.0	0.01490	0.6798	0.0117	9.75

TABLE X

EXPERIMENTAL INTERFACIAL TENSION FOR
10.3 % NORMAL-PENTANE
89.7 % PARA-XYLENE

Temp. °F.	$\frac{d_e^2}{H}$	ρ_l (gm./cm.^{3})	ρ_v (gm./cm.^{3})	γ Dynes/cm.
150.0	0.02678	0.7976	0.00128	20.90
150.0	0.02624	0.7976	0.00128	20.48
150.0	0.02772	0.7976	0.00128	21.63
150.0	0.02654	0.7976	0.00128	20.71
150.0	0.02639	0.7976	0.00128	20.60
150.0	0.02698	0.7976	0.00128	21.05
150.0	0.02694	0.7976	0.00128	21.02
150.0	0.02758	0.7976	0.00128	21.52
150.0	0.02718	0.7976	0.00128	21.21
203.5	0.02400	0.7695	0.00272	18.03
203.5	0.02320	0.7695	0.00272	17.43
203.5	0.02364	0.7695	0.00272	17.76
203.5	0.02365	0.7695	0.00272	17.77
203.5	0.02332	0.7695	0.00272	17.52
203.5	0.02416	0.7695	0.00272	18.16
203.7	0.02310	0.7694	0.00272	17.36
203.7	0.02343	0.7694	0.00272	17.61
203.7	0.02341	0.7694	0.00272	17.59
203.7	0.02385	0.7694	0.00272	17.92
203.7	0.02375	0.7694	0.00272	17.84
203.7	0.02417	0.7694	0.00272	18.16
203.7	0.02336	0.7694	0.00272	17.55
203.6	0.02361	0.7695	0.00272	17.74
203.6	0.02381	0.7695	0.00272	17.89
203.6	0.02379	0.7695	0.00272	17.87
254.8	0.02094	0.7411	0.00481	15.11
254.8	0.02049	0.7411	0.00481	14.79
254.8	0.02136	0.7411	0.00481	15.41
254.6	0.02082	0.7413	0.00481	15.02
254.6	0.02118	0.7413	0.00481	15.28
254.6	0.02067	0.7413	0.00481	14.92
254.6	0.02110	0.7413	0.00481	15.23
254.6	0.02032	0.7413	0.00481	14.67
254.6	0.02052	0.7413	0.00481	14.81
254.6	0.02153	0.7413	0.00481	15.54
255.2	0.02084	0.7409	0.00481	15.03

TABLE X (Continued)

Temp. °F	$\frac{d_e^2}{H}$	ρ_l (gm./cm^3)	ρ_v (gm./cm.^{3})	γ Dynes/cm.
255.2	0.02082	0.7409	0.00481	15.02
255.2	0.02087	0.7409	0.00481	15.06
255.2	0.02086	0.7409	0.00481	15.05
255.2	0.02138	0.7409	0.00481	15.42
255.2	0.02067	0.7409	0.00481	14.91
255.2	0.02043	0.7409	0.00481	14.74
255.2	0.02110	0.7409	0.00481	15.22
255.2	0.02076	0.7409	0.00481	14.97
300.0	0.01822	0.7147	0.00785	12.62
300.0	0.01891	0.7147	0.00785	13.10
299.5	0.01871	0.7150	0.00769	12.97
299.5	0.01855	0.7150	0.00769	12.86
299.5	0.01838	0.7150	0.00769	12.74
299.5	0.01793	0.7150	0.00769	12.43
299.3	0.01882	0.7151	0.00769	13.05
299.5	0.01838	0.7150	0.00769	12.74
299.5	0.01850	0.7150	0.00769	12.82
299.5	0.01834	0.7150	0.00769	12.71
299.6	0.01829	0.7150	0.00769	12.68
299.6	0.01875	0.7150	0.00769	13.00
299.5	0.01857	0.7150	0.00769	12.87
299.5	0.01868	0.7150	0.00769	12.95
299.5	0.01873	0.7150	0.00769	12.98
299.3	0.01869	0.7151	0.00769	12.82
302.6	0.01825	0.7131	0.00801	12.61
302.6	0.01819	0.7131	0.00801	12.57
302.6	0.01860	0.7131	0.00801	12.85
302.6	0.01826	0.7131	0.00801	12.61
351.0	0.01584	0.6828	0.0128	10.40
351.0	0.01593	0.6828	0.0128	10.46
351.0	0.01603	0.6828	0.0128	10.52
351.0	0.01603	0.6828	0.0128	10.52
350.7	0.01621	0.6830	0.0128	10.65
350.7	0.01606	0.6830	0.0128	10.55
349.8	0.01592	0.6836	0.0127	10.47
349.8	0.01601	0.6836	0.0127	10.52
350.7	0.01633	0.6830	0.0128	10.72
350.7	0.01580	0.6830	0.0128	10.38
350.8	0.01606	0.6829	0.0128	10.55
350.8	0.01613	0.6829	0.0128	10.59

TABLE X (Continued)

Temp. °F	$\frac{d_e^2}{H}$	ρ_l (gm./cm.^{3})	ρ_v (gm./cm.^{3})	γ Dynes/cm.
350.8	0.01604	0.6829	0.0128	10.54
350.8	0.01604	0.6829	0.0128	10.54
393.2	0.01361	0.6543	0.0189	8.48
393.2	0.01371	0.6543	0.0189	8.54
393.2	0.01359	0.6543	0.0189	8.46
392.8	0.01320	0.6545	0.0187	8.23
393.0	0.01328	0.6544	0.0189	8.27
392.2	0.01367	0.6550	0.0187	8.52
392.2	0.01328	0.6550	0.0187	8.28
392.2	0.01365	0.6550	0.0187	8.51
392.2	0.01354	0.6550	0.0187	8.44

TABLE XI

EXPERIMENTAL INTERFACIAL TENSION FOR
90.0 % NORMAL-PENTANE
10.0 % PARA-XYLENE

Temp. °F	$\frac{d_e^2}{H}$	ρ_l (gm./cm.^{3})	ρ_v (gm./cm.^{3})	γ Dynes/cm.
148.7	0.02013	0.6287	0.00593	12.29
148.7	0.02030	0.6287	0.00593	12.39
148.7	0.02006	0.6287	0.00593	12.24
148.8	0.02028	0.6287	0.00593	12.38
148.7	0.02025	0.6287	0.00593	12.36
148.7	0.02013	0.6287	0.00593	12.29
148.7	0.02005	0.6287	0.00593	12.24
148.5	0.02034	0.6288	0.00593	12.42
205.0	0.01586	0.5902	0.0125	8.98
205.0	0.01622	0.5902	0.0125	9.18
205.4	0.01630	0.5899	0.0127	9.22
205.4	0.01603	0.5899	0.0127	9.07
205.4	0.01599	0.5899	0.0127	9.04
205.4	0.01609	0.5899	0.0127	9.10
205.5	0.01592	0.5898	0.0127	9.00
205.5	0.01624	0.5898	0.0127	9.19
205.5	0.01601	0.5898	0.0127	9.05
230.7	0.01362	0.5710	0.0171	7.39
230.5	0.01362	0.5712	0.0170	7.40
230.5	0.01393	0.5712	0.0170	7.57
230.5	0.01399	0.5712	0.0170	7.60
230.5	0.01376	0.5712	0.0170	7.47
230.5	0.01377	0.5712	0.0170	7.48
257.0	0.01207	0.5500	0.0232	6.23
257.0	0.01205	0.5500	0.0232	6.22
256.5	0.01237	0.5505	0.0231	6.40
256.5	0.01230	0.5505	0.0231	6.36
256.5	0.01201	0.5505	0.0231	6.21
256.5	0.01210	0.5505	0.0231	6.26
256.5	0.01199	0.5505	0.0231	6.20
256.4	0.01201	0.5505	0.0231	6.21
256.2	0.01209	0.5507	0.0231	6.25
256.2	0.01204	0.5507	0.0231	6.23
256.2	0.01211	0.5507	0.0231	6.26

TABLE XII

EXPERIMENTAL INTERFACIAL TENSION
FOR NORMAL-PENTANE

Temp. °F	$\frac{d_e^2}{H}$	ρ_l (gm./cm.^{3})	ρ_v (gm./cm.^{3})	γ Dynes/cm.
150.0	0.02010	0.6017	0.00673	11.72
150.0	0.02019	0.6017	0.00673	11.77
150.0	0.01994	0.6017	0.00673	11.63
150.0	0.01976	0.6017	0.00673	11.52
150.0	0.01971	0.6017	0.00673	11.49
150.0	0.02040	0.6017	0.00673	11.89
150.0	0.01929	0.6017	0.00673	11.25
150.0	0.01936	0.6017	0.00673	11.29
150.0	0.01998	0.6017	0.00673	11.65
150.0	0.01991	0.6017	0.00673	11.61
150.0	0.01944	0.6017	0.00673	11.34
150.0	0.01975	0.6017	0.00673	11.52
150.0	0.01973	0.6017	0.00673	11.50
150.0	0.01985	0.6017	0.00673	11.58
150.0	0.01978	0.6017	0.00673	11.54
175.5	0.01789	0.5840	0.00961	10.07
175.5	0.01786	0.5840	0.00961	10.05
175.5	0.01827	0.5840	0.00961	10.29
175.5	0.01812	0.5840	0.00961	10.20
175.5	0.01806	0.5840	0.00961	10.17
175.5	0.01751	0.5840	0.00961	9.85
175.5	0.01817	0.5840	0.00961	10.23
175.5	0.01748	0.5840	0.00961	9.84
175.5	0.01774	0.5840	0.00961	9.99
201.5	0.01567	0.5648	0.0133	8.47
201.5	0.01542	0.5648	0.0133	8.34
201.5	0.01617	0.5648	0.0133	8.74
201.5	0.01579	0.5648	0.0133	8.54
201.5	0.01577	0.5648	0.0133	8.53
201.5	0.01604	0.5648	0.0133	8.67
201.5	0.01610	0.5648	0.0133	8.70
201.5	0.01562	0.5648	0.0133	8.44
201.5	0.01599	0.5648	0.0133	8.64
201.5	0.01587	0.5648	0.0133	8.58
201.5	0.01587	0.5648	0.0133	8.58

TABLE XII (Continued)

Temp. °F.	$\frac{d_e^2}{H}$	ρ_l (gm./cm.^{3})	ρ_v (gm./cm.^{3})	γ Dynes/cm.
201.5	0.01607	0.5648	0.0133	8.69
201.5	0.01544	0.5648	0.0133	8.35
201.5	0.01520	0.5648	0.0133	8.21
227.6	0.01312*	0.5443	0.0184	6.76
227.4	0.01334*	0.5445	0.0184	6.88
227.4	0.01344*	0.5445	0.0184	6.93
227.4	0.01339*	0.5445	0.0184	6.90
227.4	0.01348*	0.5445	0.0184	6.95
227.4	0.01343*	0.5445	0.0184	6.92
227.4	0.01319*	0.5445	0.0184	6.80
227.4	0.01342*	0.5445	0.0184	6.92
227.4	0.01349*	0.5445	0.0184	6.95
227.4	0.01336*	0.5445	0.0184	6.89
227.4	0.01341*	0.5445	0.0184	6.91
227.2	0.01345*	0.5446	0.0184	6.94
227.2	0.01325*	0.5446	0.0184	6.83
227.2	0.01336*	0.5446	0.0184	6.89
227.4	0.01306*	0.5445	0.0184	6.73
227.4	0.01323*	0.5445	0.0184	6.82
251.0	0.01152*	0.5245	0.0245	5.64
251.0	0.01150*	0.5245	0.0245	5.64
250.0	0.01152*	0.5254	0.0242	5.66
250.0	0.01157*	0.5254	0.0242	5.68
250.0	0.01132*	0.5254	0.0242	5.56
250.0	0.01142*	0.5254	0.0242	5.61
250.0	0.01164*	0.5254	0.0242	5.72
250.0	0.01161*	0.5254	0.0242	5.70
250.0	0.01141*	0.5254	0.0242	5.60
250.0	0.01149*	0.5254	0.0242	5.64
250.0	0.01142*	0.5254	0.0242	5.61
250.0	0.01148*	0.5254	0.0242	5.64
250.0	0.01167*	0.5254	0.0242	5.73
251.5	0.01123	0.5240	0.0245	5.50
251.5	0.01145	0.5240	0.0245	5.61
251.5	0.01148	0.5240	0.0245	5.62
251.5	0.01121	0.5240	0.0245	5.49
251.5	0.01102	0.5240	0.0245	5.40
251.5	0.01144	0.5240	0.0245	5.60
251.5	0.01143	0.5240	0.0245	5.60
251.5	0.01140	0.5240	0.0245	5.58
251.5	0.01116	0.5240	0.0245	5.46

TABLE XII (Continued)

Temp. °F.	$\frac{d_e^2}{H}$	ρ_l (gm./cm.^{3})	ρ_v (gm./cm.^{3})	γ Dynes/cm.
251.5	0.01081	0.5240	0.0245	5.29
251.5	0.01140	0.5240	0.0245	5.58
251.5	0.01115	0.5240	0.0245	5.46
251.5	0.01044	0.5240	0.0245	5.11
274.2	0.00953*	0.5031	0.0322	4.40
274.0	0.00944*	0.5033	0.0322	4.36
274.0	0.00939*	0.5033	0.0322	4.34
274.0	0.00939*	0.5033	0.0322	4.34
274.0	0.00938*	0.5033	0.0322	4.33
274.0	0.00949*	0.5033	0.0322	4.38
274.0	0.00957*	0.5033	0.0322	4.42
274.0	0.00949*	0.5033	0.0322	4.38
274.0	0.00942*	0.5033	0.0322	4.35
274.0	0.00957*	0.5033	0.0322	4.42
302.2	0.00769*	0.4740	0.0449	3.23
302.2	0.00758*	0.4740	0.0449	3.19
302.6	0.00746*	0.4735	0.0452	3.13
302.6	0.00761*	0.4735	0.0452	3.20
303.0	0.00744*	0.4731	0.0453	3.12
302.2	0.00755*	0.4740	0.0449	3.18
302.2	0.00753*	0.4740	0.0449	3.17

* Taken using a 17 gauge capillary tip. All others taken using a 15 gauge tip.

TABLE XIII

EXPERIMENTAL INTERFACIAL TENSION FOR
30.0 % ACETONE
70.0 % WATER

Temp. °F	$\frac{d_e^2}{H}$	ρ_l (gm./cm.^{3})	ρ_v (gm./cm.^{3})	γ Dynes/cm.
152.0	0.02723	0.8571	0.00113	22.84
152.0	0.02732	0.8571	0.00113	22.92
151.8	0.02691	0.8572	0.00112	22.58
151.8	0.02834	0.8572	0.00112	23.78
151.8	0.02808	0.8572	0.00112	23.56
151.8	0.02685	0.8572	0.00112	22.53
151.8	0.02769	0.8572	0.00112	23.23
151.8	0.02726	0.8572	0.00112	22.87
152.0	0.02768	0.8571	0.00113	23.22
152.0	0.02754	0.8571	0.00113	23.10
152.0	0.02802	0.8571	0.00113	23.50
152.0	0.02785	0.8571	0.00113	23.36
203.1	0.02612	0.8248	0.00230	21.05
203.1	0.02532	0.8248	0.00230	20.41
202.8	0.02506	0.8250	0.00229	20.20
202.8	0.02532	0.8250	0.00229	20.41
202.8	0.02489	0.8250	0.00229	20.07
202.8	0.02497	0.8250	0.00229	20.13
202.8	0.02520	0.8250	0.00229	20.32
202.8	0.02523	0.8250	0.00229	20.34
202.8	0.02515	0.8250	0.00229	20.28
202.8	0.02492	0.8250	0.00229	20.09
202.8	0.02484	0.8250	0.00229	20.03
203.0	0.02501	0.8248	0.00230	20.16
203.0	0.02460	0.8248	0.00230	19.83
256.6	0.02164	0.7891	0.00476	16.63
256.6	0.02205	0.7891	0.00476	16.95
256.6	0.02245	0.7891	0.00476	17.26
256.7	0.02225	0.7890	0.00477	17.10
256.7	0.02175	0.7890	0.00477	16.72
256.8	0.02256	0.7889	0.00478	17.34
256.8	0.02201	0.7889	0.00478	16.91
252.8	0.02148	0.7917	0.00455	16.57
252.8	0.02099	0.7917	0.00455	16.19
252.7	0.02165	0.7917	0.00455	16.70
252.7	0.02113	0.7917	0.00455	16.30

TABLE XIII (Continued)

Temp. °F	$\frac{d_e^2}{H}$	ρ_l (gm./cm^3)	ρ_v (gm./cm.^{3})	γ Dynes/cm.
252.6	0.02170	0.7918	0.00455	16.74
252.6	0.02154	0.7918	0.00455	16.62
252.6	0.02125	0.7918	0.00455	16.40
304.0	0.01859	0.7554	0.00843	13.61
304.0	0.01879	0.7554	0.00843	13.75
304.0	0.01843	0.7554	0.00843	13.49
304.0	0.01845	0.7554	0.00843	13.51
304.0	0.01865	0.7554	0.00843	13.65
304.0	0.01885	0.7554	0.00843	13.80
304.0	0.01883	0.7554	0.00843	13.78
355.5	0.01601	0.7159	0.0146	11.00
355.5	0.01546	0.7159	0.0146	10.63
354.6	0.01623	0.7166	0.0145	11.17
354.6	0.01597	0.7166	0.0145	10.99
354.6	0.01617	0.7166	0.0145	11.13
354.2	0.01623	0.7169	0.0144	11.17
354.2	0.01597	0.7169	0.0144	10.99
355.5	0.01604	0.7159	0.0146	11.02
355.5	0.01618	0.7159	0.0146	11.12
355.5	0.01590	0.7159	0.0146	10.93
355.5	0.01598	0.7159	0.0146	10.98
355.5	0.01606	0.7159	0.0146	11.04
379.6	0.01476	0.6961	0.0186	9.80
379.6	0.01487	0.6961	0.0186	9.87
379.6	0.01433	0.6961	0.0186	9.51
379.6	0.01461	0.6961	0.0186	9.70
379.6	0.01469	0.6961	0.0186	9.75

TABLE XIV

EXPERIMENTAL INTERFACIAL TENSION FOR
70.0 % ACETONE
30.0 % WATER

Temp. °F.	$\frac{d_e^2}{H}$	ρ_l (gm./cm^3)	ρ_v (gm./cm^3)	γ Dynes/cm.
154.1	0.02537	0.7714	0.00233	19.12
154.1	0.02467	0.7714	0.00233	18.59
154.1	0.02539	0.7714	0.00233	19.14
154.1	0.02525	0.7714	0.00233	19.03
154.1	0.02537	0.7714	0.00233	19.12
154.1	0.02544	0.7714	0.00233	19.17
154.1	0.02551	0.7714	0.00233	19.23
154.1	0.02517	0.7714	0.00233	18.97
154.0	0.02522	0.7715	0.00233	19.01
154.0	0.02540	0.7715	0.00233	19.15
154.0	0.02472	0.7715	0.00233	18.63
203.1	0.02238	0.7376	0.00481	16.07
203.1	0.02127	0.7376	0.00481	15.28
203.2	0.02207	0.7375	0.00483	15.85
203.4	0.02241	0.7374	0.00484	16.09
203.4	0.02255	0.7374	0.00484	16.19
203.4	0.02190	0.7374	0.00484	15.72
203.4	0.02222	0.7374	0.00484	15.95
203.4	0.02157	0.7374	0.00484	15.48
203.4	0.02231	0.7374	0.00484	16.02
252.1	0.01904	0.7013	0.00934	12.91
252.1	0.01926	0.7013	0.00934	13.06
252.1	0.01930	0.7013	0.00934	13.09
252.1	0.01892	0.7013	0.00934	12.83
252.1	0.01828	0.7013	0.00934	12.40
252.1	0.01830	0.7013	0.00934	12.41
252.1	0.01878	0.7013	0.00934	12.74
252.1	0.01867	0.7013	0.00934	12.66
252.1	0.01847	0.7013	0.00934	12.53
252.1	0.01879	0.7013	0.00934	12.74
252.1	0.01883	0.7013	0.00934	12.77
252.1	0.01917	0.7013	0.00934	13.00
303.6	0.01530	0.6596	0.0171	9.63
303.6	0.01545	0.6596	0.0171	9.73
303.6	0.01528	0.6596	0.0171	9.62

TABLE XIV (Continued)

Temp. °F.	$\frac{d_e^2}{H}$	ρ_l (gm./cm^3)	ρ_v (gm./cm.^{3})	γ Dynes/cm.
303.6	0.01545	0.6596	0.0171	9.73
303.6	0.01554	0.6596	0.0171	9.78
303.6	0.01526	0.6596	0.0171	9.61
303.6	0.01539	0.6596	0.0171	9.69
303.6	0.01546	0.6596	0.0171	9.73
303.6	0.01514	0.6596	0.0171	9.53
303.6	0.01516	0.6596	0.0171	9.54
303.6	0.01522	0.6596	0.0171	9.58
330.0	0.01294	0.6362	0.0231	7.78
330.0	0.01271	0.6362	0.0231	7.64
330.3	0.01324	0.6359	0.0232	7.95
330.3	0.01307	0.6359	0.0232	7.85
330.3	0.01335	0.6359	0.0232	8.02
330.3	0.01319	0.6359	0.0232	7.92
330.3	0.01334	0.6359	0.0232	8.01
330.3	0.01314	0.6359	0.0232	7.89
330.3	0.01325	0.6359	0.0232	7.96
330.3	0.01327	0.6359	0.0232	7.97
330.4	0.01381	0.6359	0.0232	8.29
330.3	0.01335	0.6359	0.0232	8.02
330.4	0.01330	0.6359	0.0232	7.99
358.2	0.01107	0.6093	0.0311	6.27
358.1	0.01110	0.6094	0.0311	6.29
358.1	0.01123	0.6094	0.0311	6.37
358.1	0.01104	0.6094	0.0311	6.26
358.2	0.01132	0.6093	0.0311	6.42
358.2	0.01110	0.6093	0.0311	6.29
358.2	0.01106	0.6093	0.0311	6.27
358.2	0.01130	0.6093	0.0311	6.40
358.2	0.01127	0.6093	0.0311	6.39
358.1	0.01104	0.6094	0.0311	6.26
358.1	0.01114	0.6094	0.0311	6.31
358.1	0.01121	0.6094	0.0311	6.35
358.1	0.01132	0.6094	0.0311	6.42
358.1	0.01154	0.6094	0.0311	6.54
358.0	0.01145	0.6095	0.0310	6.49
358.0	0.01152	0.6095	0.0310	6.53
384.0	0.00907	0.5824	0.0407	4.82
383.5	0.00895	0.5830	0.0405	4.76

TABLE XIV (Continued)

Temp. °F.	$\frac{d_e^2}{H}$	ρ (gm./cm.^{3})	ρ (gm./cm.^{3})	γ Dynes/cm.
383.5	0.00909	0.5830	0.0405	4.83
383.5	0.00907	0.5830	0.0405	4.82
383.8	0.00925	0.5826	0.0407	4.91
384.0	0.00905	0.5824	0.0407	4.81
384.0	0.00902	0.5824	0.0407	4.79
384.0	0.00928	0.5824	0.0407	4.93

TABLE XV

EXPERIMENTAL INTERFACIAL TENSION
FOR ACETONE

Temp. °F.	$\frac{d_e^2}{H}$	ρ_l (gm./cm.^{3})	ρ_v (gm./cm.^{3})	γ Dynes/cm.
149.0	0.02509	0.7345	0.00298	17.99
149.0	0.02465	0.7345	0.00298	17.67
149.0	0.02433	0.7345	0.00298	17.44
149.0	0.02462	0.7345	0.00298	17.65
149.0	0.02456	0.7345	0.00298	17.61
149.0	0.02463	0.7345	0.00298	17.66
149.0	0.02430	0.7345	0.00298	17.42
149.0	0.02446	0.7345	0.00298	17.54
149.0	0.02450	0.7345	0.00298	17.56
149.0	0.02458	0.7345	0.00298	17.62
204.1	0.02043	0.6943	0.00663	13.77
204.0	0.02006	0.6943	0.00661	13.52
204.1	0.02001	0.6943	0.00663	13.48
204.1	0.02043	0.6943	0.00663	13.77
204.1	0.02067	0.6943	0.00663	13.93
204.1	0.02047	0.6943	0.00663	13.79
204.1	0.02033	0.6943	0.00663	13.70
204.1	0.02051	0.6943	0.00663	13.82
204.1	0.02023	0.6943	0.00663	13.63
258.6	0.01606	0.6504	0.0143	10.01
258.6	0.01598	0.6504	0.0143	9.96
258.5	0.01605	0.6504	0.0143	10.01
258.5	0.01594	0.6504	0.0143	9.94
258.5	0.01567	0.6504	0.0143	9.77
258.5	0.01575	0.6504	0.0143	9.82
258.4	0.01601	0.6505	0.0143	9.98
258.5	0.01577	0.6504	0.0143	9.83
258.5	0.01591	0.6504	0.0143	9.92
259.2	0.01593	0.6498	0.0143	9.92
259.2	0.01657	0.6498	0.0143	10.32
302.8	0.01268	0.6054	0.0259	7.20
303.0	0.01292	0.6103	0.0244	7.42
303.0	0.01270	0.6103	0.0244	7.29
303.2	0.01277	0.6101	0.0245	7.33

TABLE XV (Continued)

Temp. °F.	$\frac{d_e^2}{H}$	ρ_l (gm./cm.^{3})	ρ_v (gm./cm.^{3})	γ Dynes/cm.
303.2	0.01297	0.6101	0.0245	7.44
303.2	0.01286	0.6101	0.0245	7.38
303.2	0.01277	0.6101	0.0245	7.33
303.2	0.01288	0.6101	0.0245	7.39
303.2	0.01283	0.6101	0.0245	7.36
303.4	0.01287	0.6099	0.0245	7.38
397.7	0.01266	0.6057	0.0258	7.20
307.7	0.01273	0.6057	0.0258	7.24
307.8	0.01202	0.6056	0.0259	6.83
308.0	0.01268	0.6054	0.0259	7.20
309.0	0.01263	0.6045	0.0262	7.16
309.0	0.01257	0.6045	0.0262	7.12
308.8	0.01220	0.6046	0.0261	6.92
308.8	0.01234	0.6046	0.0261	7.00
308.8	0.01258	0.6046	0.0261	7.13
308.8	0.01249	0.6046	0.0261	7.08
308.8	0.01252	0.6046	0.0261	7.10
333.8	0.01076	0.5791	0.0348	5.74
333.8	0.01015	0.5791	0.0348	5.41
333.8	0.01063	0.5791	0.0348	5.67
334.0	0.01061	0.5789	0.0349	5.66
334.5	0.01064	0.5783	0.0351	5.66
334.0	0.01055	0.5789	0.0349	5.62
334.0	0.01068	0.5789	0.0349	5.69
329.9	0.01072	0.5832	0.0333	5.78
329.9	0.01062	0.5832	0.0333	5.72
330.0	0.01075	0.5831	0.0334	5.79
329.8	0.01080	0.5833	0.0333	5.82
329.7	0.01121	0.5834	0.0332	6.04
329.7	0.01085	0.5834	0.0332	5.85
329.5	0.01092	0.5836	0.0332	5.89
329.5	0.01082	0.5836	0.0332	5.84
329.6	0.01095	0.5835	0.0332	5.91
329.2	0.01102	0.5840	0.0331	5.95
329.6	0.01103	0.5835	0.0332	5.95
358.0	0.00885	0.5517	0.0457	4.39
357.6	0.00858	0.5522	0.0454	4.26
357.8	0.00882	0.5519	0.0456	4.38

TABLE XV (Continued)

Temp. °F	$\frac{d_e^2}{H}$	ρ_l (gm./cm.^{3})	ρ_v (gm./cm.^{3})	γ Dynes/cm.
357.2	0.00893	0.5527	0.0452	4.44
357.2	0.00909	0.5527	0.0452	4.52
357.2	0.00908	0.5527	0.0452	4.52
358.1	0.00898	0.5516	0.0458	4.45
358.2	0.00878	0.5515	0.0459	4.35
358.1	0.00879	0.5516	0.0458	4.36
357.8	0.00883	0.5519	0.0456	4.38
357.8	0.00894	0.5519	0.0456	4.44
357.8	0.00891	0.5519	0.0456	4.42
382.4	0.00657	0.5203	0.0605	2.96

APPENDIX E

ESTIMATE OF ERROR

ESTIMATE OF ERROR

The work of Deam (4), following the approach of previous authors, developed expressions for the most probable value of error in interfacial tension as a result of uncertainties in experimentally determined quantities. As the approach to the determination of interfacial tension was similar to that used by Deam, these expressions were adopted for use in this work. The expressions for the error in interfacial tension resulting from errors in the gravitational constant (16), density difference (17), equatorial diameter (18), and selected plane diameter (19) were given as indicated in the following equations.

Gravitational constant:

$$\gamma_g = \left(\frac{\partial \gamma}{\partial g}\right)\delta_g = \left(\Delta\rho\left(\frac{1}{H}\right)d_e^{\,2}\right)\delta_g = \left(\frac{\gamma}{g}\right)\delta_g \qquad (16)$$

Density difference:

$$\gamma_{\Delta\rho} = \left(\frac{\partial \gamma}{\partial \Delta\rho}\right)\partial_{\Delta\rho} = \left(g\left(\frac{1}{H}\right)d_e^{\,2}\right)\delta_{\Delta\rho} = \left(\frac{\gamma}{\Delta\rho}\right)\delta_{\Delta\rho} \qquad (17)$$

Equatorial diameter:

$$\gamma_{d_e} = \left(\frac{\partial \gamma}{\partial d_e}\right)\delta_{d_e} = 4.6444\left(\frac{\gamma}{d_e}\right)\delta_{d_e} \qquad (18)$$

Selected plane diameter:

$$\gamma_{d_s} = \left(\frac{\partial \gamma}{\partial d_s}\right)\delta_{d_s} = -2.6444\left(\frac{\gamma}{d_s}\right)\delta_{d_s} \qquad (19)$$

The most probable value of error in interfacial tension was given as a function of these errors, as expressed in equation (20). From this expression, the most probable error was computed using typical

$$\Delta\gamma = \left(\gamma_g^2 + \gamma_{\Delta\rho}^2 + \gamma_{d_s}^2 + \gamma_{d_s}^2\right)^{1/2} \qquad (20)$$

values of the experimentally measured quantities. The errors in these quantities were taken as the smallest reasonable errors to be expected, in order to arrive at an estimate of the limiting accuracy of the work. The values for a set of data taken for the mixture of 10.3 mole per cent normal-pentane in para-xylene are

$$d_e = 0.2161 \text{ cm.}$$

$$d_s = 0.1967 \text{ cm.}$$

$$\Delta\rho = 0.7068 \text{ gm./c.c.}$$

$$g = 980 \text{ cm./sec.}^2$$

$$\gamma = 12.96 \text{ dynes/cm.}$$

The following uncertainties were assumed:

$$\delta_g = 0 \text{ cm./sec.}^2$$

$$\delta_{\Delta\rho} = 0.007 \text{ gm./c.c.}$$

$$\delta_{d_e} = 0.001 \text{ cm.}$$

$$\delta_{d_s} = 0.001 \text{ cm.}$$

From equation (20), the most probable value of error in interfacial tension is

$$\Delta\gamma = 0.35 \text{ dynes/cm.}$$

and for the particular data point considered,

$$\gamma = 12.96 \pm 0.35 \text{ dynes/cm.}$$

VITA

Michael Brant Miller

Candidate for the Degree of

Master of Science

Thesis: EXPERIMENTAL DETERMINATION OF THE INTERFACIAL TENSION OF BINARY SYSTEMS

Major Field: Chemical Engineering

Biographical:

Personal Data: Born in Tulsa, Oklahoma, August 19, 1943, the son of Mr. and Mrs. Arthur Miller Jr.; Married to Aneta Louise Smith, August 22, 1964.

Education: Graduated from Thomas Alva Edison High School, Tulsa, Oklahoma, in May, 1961; entered undergraduate engineering program at Washington University, St. Louis, Missouri in September, 1961; received Bachelor of Science degree in Chemical Engineering from Oklahoma State University in May, 1970; completed requirements for degree of Master of Science at Oklahoma State University in May, 1972.

Membership in Scholarly or Professional Societies: Omega Chi Epsilon, associate member of National Society of Professional Engineers and Oklahoma Society of Professional Engineers.

Professional Experience: Graduate research assistant and graduate teaching assistant, School of Chemical Engineering, Oklahoma State University, 1970-1972; registered Engineer-in-Training in the State of Oklahoma, 1971-1972.